[31] V. K. Prasanna and A. S. Rao. Parallel orientation of polygonal parts. IEEE *Transactions on Robotics and Automation*, 8(5):678–687, October 1992. Preliminary version presented at the Int. Conf. on Parallel Processing, August 1992.

[32] V. T. Rajan, R. Burridge, and J. T. Schwartz. Dynamics of a rigid body in frictional contact with rigid walls. In IEEE *International Conference on Robotics and Automation*, 1987.

[33] A. S. Rao. *Algorithmic Plans for Robotic Manipulation*. PhD thesis, University of Southern California, Department of Electrical Engineering–Systems, December 1992.

[34] A. S. Rao. Feeding planar parts with a parallel jaw gripper. In *International Conference on Robotics and Manufacturing*, Oxford, England, September 1993. IASTED.

[35] A. S. Rao and K. Y. Goldberg. Grasping planar curved parts with a parallel-jaw gripper. Technical Report # 299, University of Southern California, Institute of Robotics and Intelligent Systems (IRIS), Los Angeles, Calif. 90089-0273, September 1991.

[36] A. S. Rao and K. Y. Goldberg. Orienting generalized polygonal parts. In *International conference on Robotics and Automation* (ICRA), Nice, France, May 1992. IEEE.

[37] A. S. Rao and K. Y. Goldberg. Shape from diameter: recognizing polygonal parts with a parallel-jaw gripper. *International Journal of Robotics Research*, 13(1), February 1994. (to appear).

[38] F. Reuleaux. *The Kinematics of Machinery*. Macmilly and Company, 1876. Republished by Dover in 1963.

[39] A. A. Schaeffer and C. J. Van Wyk. Convex hulls of piecewise-smooth Jordan curves. *Journal of Algorithms*, 8(1):66–94, 1987.

[40] R. H. Taylor, M. T. Mason, and K. Y. Goldberg. Sensor-based manipulation planning as a game with nature. In *Fourth International Symposium on Robotics Research*, August 1987.

[41] J. C. Trinkle and R. P. Paul. Planning for dextrous manipulation with sliding contacts. *International Journal of Robotics Research*, June 1990.

[42] J. D. Wolter, R. A. Volz, and A. C. Woo. Automatic generation of gripping positions. IEEE *Transactions on Systems, Man, and Cybernetics*, SMC-15, March/April 1985.

[43] I. M. Yaglom and V.G. Boltyanskii. *Convex Figures*. Holt, Rinehart and Winston, New York, 1951.

[14] K. Y. Goldberg. Orienting polygonal parts without sensors. *Algorithmica*, 10(2):201–225, Aug 1993. (Special issue on Computational Robotics).

[15] R. A. Grupen, T. C. Henderson, and I. D. McCammon. A survey of general purpose manipulation. *International Journal of Robotics Research*, 8(1), 1989.

[16] C. M. Hoffmann. *Geometric and Solid Modeling: An Introduction*. Computer Graphics and Geometric Modeling. Morgan Kaufmann, San Mateo, CA 94403., 1989.

[17] J. Jameson. *Analytic Techniques for Automated Grasp*. PhD thesis, Department of Mechanical Engineering, Stanford University, June 1985.

[18] K. Lynch. The mechanics of fine manipulation by pushing. In *International Conference on Robotics and Automation*. IEEE, May 1992.

[19] M. Mani and R. D. W. Wilson. A programmable orienting system for flat parts. In *Proc: North American Mfg. Research Inst. Conf XIII*, 1985.

[20] X. Markenscoff, L. Ni, and C. H. Papadimitriou. The geometry of grasping. *International Journal of Robotics Research*, 9(1), February 1990.

[21] M. T. Mason. *Manipulator Grasping and Pushing Operations*. PhD thesis, MIT, June 1982. published in *Robot Hands and the Mechanics of Manipulation*, MIT Press, 1985.

[22] M. T. Mason. On the scope of quasi-static pushing. In O. Faugeras and G. Giralt, editors, *The Third International Symposium on Robotics Research*. MIT Press, 1986.

[23] M. T. Mason. Kicking the sensing habit. In *Asilomar Winter Workshop*. AAAI, November 1991.

[24] M. T. Mason, K. Y. Goldberg, and R. H. Taylor. Planning sequences of squeeze-grasps to orient and grasp polygonal objects. Technical Report CMU-CS-88-127, Carnegie Mellon University, Computer Science Dept., Pittsburgh, PA 15213, April 1988.

[25] A. Mottaez, M. Coutinho, and K. Y. Goldberg. Positioning polygonal parts without sensors. In *Sensors and Controls for Automated Manufacturing Systems*. SPIE, September 1993.

[26] B. K. Natarajan. Some paradigms for the automated design of parts feeders. *International Journal of Robotics Research*, 8(6):98–109, December 1989. Also appeared in IEEE FOCS, 1986.

[27] E. N. Ohwovoriole. Kinematics and friction in grasping by robotic hands. *Transactions of the ASME*, 109, 1987.

[28] J. Pertin-Troccaz. Grasping: A state of the art. In *The Robotics Review I*, pages 71–98. MIT Press, 1989. edited by O. Khatib, J. J. Craig, and T. Lozano-Perez.

[29] M. A. Peshkin. *Planning Robotic Manipulation Strategies for Sliding Objects*. PhD thesis, Carnegie-Mellon University, Department of Physics, Pittsburgh, Pennylvania, Nov 1986. Also published as a book: *Robotic Manipulation Strategies*, Prentice Hall, 1990, New Jersey.

[30] M. A. Peshkin and A. C. Sanderson. Planning robotic manipulation strategies for workpieces that slide. *IEEE Journal of Robotics and Automation*, 4(5), October 1988.

C Composing Grasp Functions

Here we prove the following.

Lemma 5 *Given two monotonic functions f, g whose domain and range are S^1. f (resp. g) is made up of n (resp. m) steps and ramps, each step having a fixed point. Then $h = f \circ g$ is also a monotonic function whose domain and range is S^1 and is made up of at most $\max(m, n)$ ramps and steps, each step having a fixed point.*

Proof: First notice the simple fact that for any $S \subseteq S^1$, and if $f(S)$ denotes $\mathrm{HULL}(\{f(x)|x \in S\})$, then $f(S) \subseteq \mathrm{HULL}(S)$. Similarly for $g(S)$. This follows from the specification of f, g. Now let $S = [x, y)$ be a step in f with fixed point α. Since $g(S) \subseteq S$, we have that $h(S) = f(S) = \alpha$. If $S = [x, y)$ is a ramp in f, then clearly $h(S) = g(S) = S$. The claims all follow from these two statements. $\square$

References

[1] R. V. Benson. *Euclidian Geometry and Convexity*. McGraw-Hill Book Company, 1966.

[2] R. C. Brost. Automatic grasp planning in the presence of uncertainty. *The International Journal of Robotics Research*, 8(1), February 1988.

[3] R. C. Brost and M. T. Mason. Graphical analysis of planar rigid-body dynamics with multiple frictional contacts. In *5th International Symposium on Robotics Research*, 1989.

[4] V. Chandru and R. Venkataraman. Circular hulls and Orbiforms of simple polygons. In *Symposium on Discrete Algorithms* (SODA). SIAM-ACM, 1991.

[5] B. Chazelle. Triangulating a simple polygon in linear time. *Discrete and Computational Geometry*, 6:485–524, 1991.

[6] Y-B. Chen and D. J. Ierardi. Oblivious plans for orienting and distinguishing polygonal parts. In *The 4th Canadian Conference on Computational Geometry*, 1992.

[7] D. P. Dobkin and D. L. Souvaine. Computational geometry in a curved world. *Algorithmica*, pages 421–457, 1990.

[8] H. Edelsbrunner. *Algorithms in Combinatorial Geometry*. EATCS Monographs on Theoretical Computer Science. Springer-Verlag, Berlin, 1987.

[9] D. Eppstein. Reset sequences for monotonic automata. *SIAM Journal of Computing*, 19(3), 1990.

[10] M. A. Erdmann. On motion planning with uncertainty. Master's thesis, MIT, August 1984.

[11] M. A. Erdmann, M. T. Mason, and G. Vaneček Jr. Mechanical parts orienting: The case of a polyhedron on a table. In *International Conference on Robotics and Automation*. IEEE, April 1991.

[12] R. S. Fearing. Simplified grasping and manipulation with dextrous robot hands. *IEEE Journal of Robotics and Automation*, RA-2(4), December 1986.

[13] K. Y. Goldberg. A kinematically-yielding gripper. In *22nd International Symposium on Industrial Automation*, October 1991.

Figure 20: Modifying the grasp function after the three grasps. At the top is a typical diameter function shown with a classification of its equilibrium orientations. Steps and ramps are shown side-by-side for convenience. (a) shows the single-grasp grasp function. Notice that steps are open, ramps are closed, and isolated points exist (at local maxima orientations). (b) shows the desired grasp function with all steps and ramps being left-closed and right-open and no isolated points. (c) shows the modified grasp grasp function which has left-closed and right-open steps and ramps and matches the one in (b) except at $(0, +)$ orientations at which they differ according to δ. However, δ is a parameter of the modified grasp and maybe chosen arbitrarily small.

For examples of these orientations, see Fig. 19. In Fig. 12, α is a stable equilibrium orientation and x is an unstable equilibrium orientation. Orientations strictly within (u, v) are neutral equilibrium orientations. Orientations strictly within (x, u), except for α are unstable orientations, while u and v are semiunstable.

In the terminology defined in this section, consider once again the derivation of Γ from d earlier discussed in Section 2.1.2. First every region (u, v) of neutral orientations results in a ramp (u, v). Now ignore neutral orientations while treating semistable equilibrium orientations as stable equilibrium orientations and semiunstable ones as unstable equilibrium orientations. Therefore, we only have stable and unstable equilibrium orientations in addition to unstable orientations. If u is an unstable equilibrium orientation and the first stable equilibrium orientation to its right (*resp.*left) is x, then the orientations (u, x) (*resp.*(x, u)) results in part of a step with fixed point v. (Finally, make all steps and ramps left-closed, right-open justified by the modified grasping process of Appendix B.)

B   Justifying Left-close and Right-Open Steps and Ramps

Here we prove that steps and ramps can be assumed left-closed, right-open by a change to the grasping process replacing every grasp by three "mini-grasps."

Consider Γ derived faithfully from Fact 1. Such a grasp function satisfies $\Gamma(\theta) = \theta$ if and only if θ is an equilibrium orientation. In particular $\Gamma(\theta) = \theta$ for semistable, semiunstable and unstable equilibrium orientations. This results in possibly open steps and closed (at both ends) ramps and isolated points. See Fig. 20(a). We show below how to modify the grasping process so that all steps and ramps become left-closed and right-open (and isolated points disappear). This is important from the point of view of the completeness proofs of the planning algorithm in Section 4.2.

Every grasp action at angle α is replaced by three "minor" grasp actions in the sequence $\alpha, -\delta, +\delta$, where δ is a small positive orientation depending on the diameter function. Specifically, we can choose δ as any positive real number less than

$$\min\{|\theta_a - \theta_b|\}$$

where θ_a ranges over all stable equilibrium orientations and θ_b are adjacent unstable equilibrium orientations to θ_a. Consider semistable orientations as stable, and semiunstable orientations as unstable equilibrium orientations in this computation of d.

If α was an unstable orientation, or a stable equilibrium orientation, or a $(-, 0)$ semistable orientation (as defined in Appendix A) then notice that the sequence of three grasps is equivalent to grasp at α. This is clearly true for the first two types of orientations. For the third $((-, 0)$ semistable orientations), just notice that the third grasp nullifies the action of the second.

However, if α were a semiunstable or unstable equilibrium orientation, then the first grasp results in orientation $\Gamma(\alpha) = \alpha$. For the second grasp we turn the jaws by $-\delta$, which is equivalent to the situation where the part is rotated $+\delta$ before grasping. The final orientation after this grasp is $\Gamma(\alpha + \delta)$. The third grasp does not change this orientation unless we have a $(+, 0)$ semiunstable orientation in which case the third grasp merely reverses the effect of the second.

Finally consider the case of $(0, +)$ semistable orientations. It has a step to its right and a ramp to its left. The sequence of three grasp actions locally changes the grasp function so that the step is increased in extent by δ and the ramp is reduced by the same amount.

See Fig. 20. The grasp function resulting from the three grasps consists of left-closed ramps and steps and differs from the desired grasp function only at $(0, +)$ semistable orientations as described above. It may be seen that the length of the plan for the grasp function shown in Fig. 20(b) is no larger than that in (c).
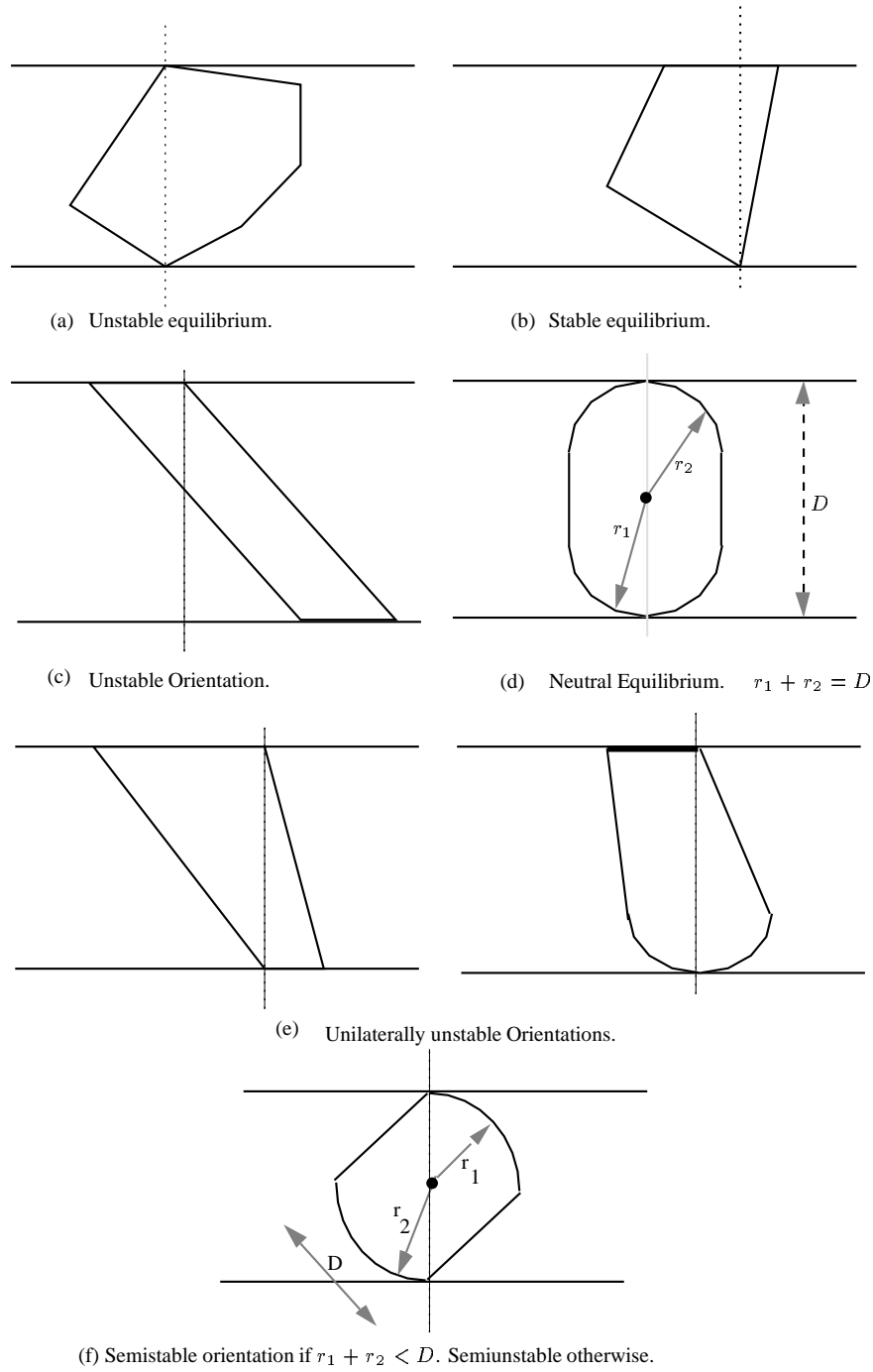
(a) Unstable equilibrium.

(b) Stable equilibrium.

(c) Unstable Orientation.

(d) Neutral Equilibrium. $r_1 + r_2 = D$

(e) Unilaterally unstable Orientations.

(f) Semistable orientation if $r_1 + r_2 < D$. Semiunstable otherwise.

Figure 19: A classification of orientations.

30

on stable orientations corresponding to polygon edges. As we have seen, the generalization required us to consider uncountable sets of possible stable states and prevented us from establishing a combinatorial bound on the length of the grasp plan. But we have proved that a plan exists for any algebraic part. Erdmann, Mason, and Vanacek [11] recently commented that proving a grasp plan exists for any polygonal part "is perhaps the first characterization of a class of manipulable parts". This paper characterizes the much broader class of algebraic parts as manipulable.

The Appendix

A A Classification of Orientations in terms of Grasp Stability

In this section, we classify contact or grasped states into several categories (see Fig. 19) on basis of the behavior of Γ around θ, *i.e.* on how stable an orientation is to the grasping process.

- *Equilibrium orientations*: Orientations θ of P wrt G that are such that $\Gamma(\theta) = \theta$, *i.e.* such orientations are not changed by the grasping. These are further subdivided into –

  1. *Stable equilibrium*: $\Gamma(\theta \pm \delta) = \theta$.
  2. *Neutral equilibrium*: $\Gamma(\theta \pm \delta) = \theta \pm \delta$.
  3. *Unstable equilibrium*: $\Gamma(\theta \pm \delta) \neq \theta, \theta \pm \delta$.
  4. *Semistable equilibrium*: $\Gamma(\theta + \delta) = \theta + \delta$ and $\Gamma(\theta - \delta) = \theta$ (or vice versa, *i.e.* interchanging $+, -$). Such orientations are neutral for infinitesimal rotations in a particular direction while stable in the other direction.
  5. *Semiunstable equilibrium*: These are orientations θ that are neutral wrt (infinitesimal) rotations in one direction while unstable wrt the other direction. That is, $\Gamma(\theta + \delta) = \theta + \delta$ and $\Gamma(\theta - \delta) \neq \theta, \theta - \delta$ (or vice versa by interchanging $+, -$).

- *Unstable orientations* (distinct from unstable *equilibrium* orientations.) Orientations θ such that $\Gamma(\theta) \neq \theta$.

The diameter function can be likened to the energy of the system in the following sense : stable equilibrium (*resp.* unstable equilibrium) orientations are precisely the local minima (*resp.* local maxima) orientations in the diameter function; and neutral (*resp.* semistable, semiunstable) orientations are those at the interior (*resp.* end-points) of a region of constant diameter.

Let d' refer to the first derivative of d. The quantity δ, may be chosen so that $d'(\theta - \delta)$ and $d'(\theta + \delta)$ are both defined. That the above is an exhaustive set of orientations is made clear by considering the signs ($+, -$ or 0) of the pair of numbers $(d'(\theta - \delta), d'(\theta + \delta))$: Unstable orientations are $(+, +)$ or $(-, -)$ orientations; neutral equilibrium orientations are $(0, 0)$; stable equilibrium $(-, +)$; unstable equilibrium $(+, -)$; semistable $(-, 0)$ or $(0, +)$; and finally semiunstable orientations are $(+, 0)$ or $(0, -)$.
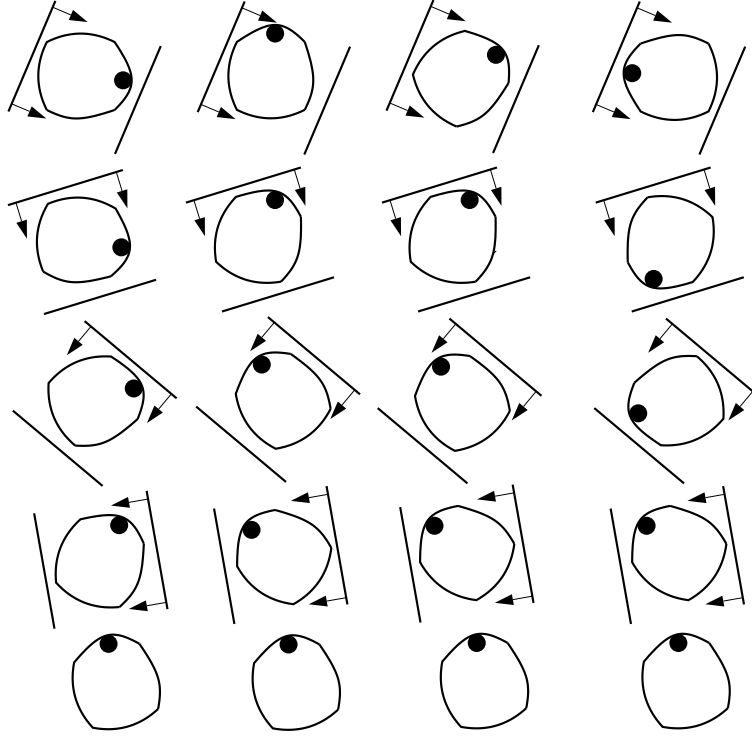
Figure 18: Top view of a four-stage plan for orienting the part in Fig. 8 into a unique orientation using push-grasp actions. Four traces are shown, one per column. Note that while the first and fourth columns begin 180 degrees apart here they end up in the same orientation (compare with Fig. 10).
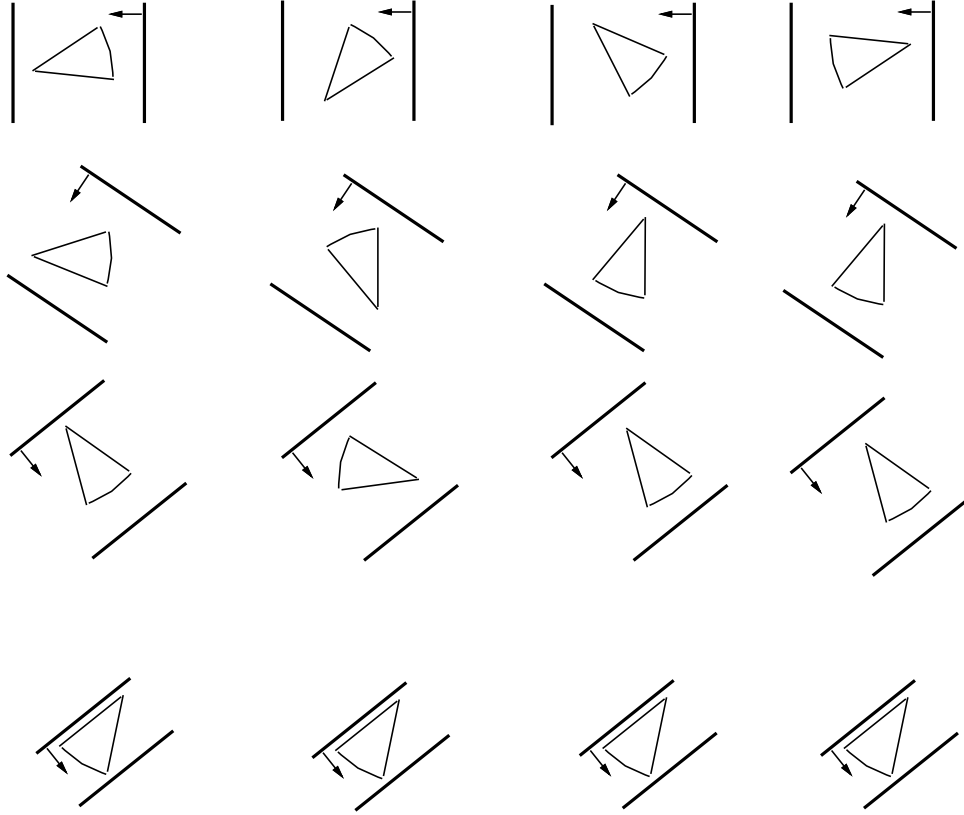
28

Figure 17: Four traces of 3-step push-grasp plan. The push angles are $0, -56, -128$ degrees. Line with arrow indicates pushing jaw. The initial orientations for the four traces are same as those in Fig. 2. Notice the final orientations in both figures. Initial orientations that are $180°$ apart (see the first and fourth columns in Fig. 2), end up $180°$ apart in Fig. 2 (squeeze-grasp actions). However, in this figure, they end up in the identical orientation. Push-grasping resolves the ambiguity.

push-grasp function instead of the squeeze-grasp function. An example for the pie-shaped part is shown in Fig.s 16 and 17. Another example (algebraic part of Fig. 8) is in Fig. 18. Since the push-grasp function has period 2π unless the part has rotational symmetry, The resulting push-grasp plans allow us to eliminate the $180°$ ambiguity in the part's final orientation that is inherent with squeeze-grasp plans. The correctness, complexity and completeness of the algorithm can be proved as before.
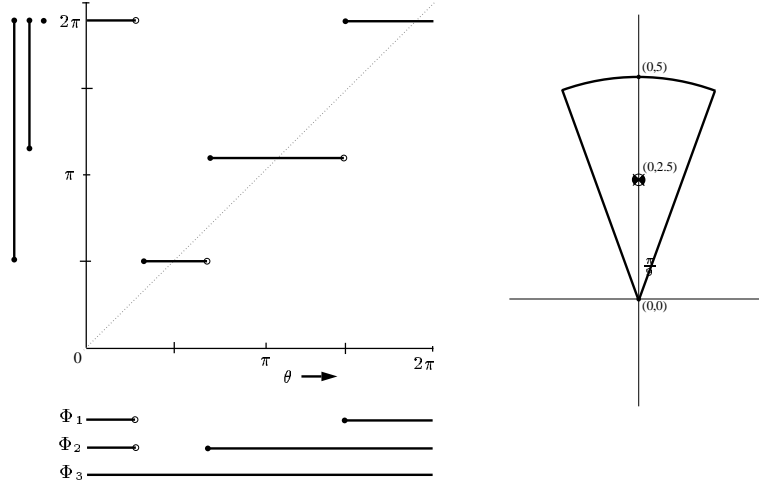

Figure 16: The push-grasp function (left) for the pie-shaped part (right). The part is a $40°$ sector of a circle of radius 5. Its center of mass is assumed to be at the point $(0, 2.5)$. The planning algorithm finds intervals Φ_1, Φ_2, Φ_3 corresponding to the horizontal bars below the push-grasp function.

6 Discussion

We started with the assumption that the part's initial orientation is unknown and that the part will rotate during grasping. For the class of algebraic parts, we showed that part motion during grasping can be described with a function consisting only of steps and ramps. Based on this, we showed that a grasp plan exists for any algebraic part and gave a efficient algorithm for finding the shortest grasp plan. These grasp plans do not rely on sensors to resolve uncertainty. Instead, they use the geometry of the gripper and part to guide passive mechanical compliance [23].

We have not addressed the problem of computing grasp functions in this paper. In [35], we gave an $O(n)$ algorithm for computing the grasp function of a part bounded by n linear and circular arcs. For algebraic parts, [34] presents the general equations required to compute the extrema in its diameter and radius functions. This is sufficient to compute the squeeze-grasp and push-grasp functions.

Not all industrial parts can be treated as planar; we assumed that part motion is confined to the plane. We restricted part boundaries to be algebraic to establish finite complexity of the grasp functions for Theorem 1. As noted, "this class is very rich and includes most of the curves and surfaces used in engineering design" [16]. However, not all parts are algebraic. Examples are the helix and the exponential curve found in some sea shells. However, as long as the grasp function of a part is known and finite, the algorithm reported here will find a grasp plan.

Certainly it is true that any curved part can be approximated with a polygon. Yet it is not obvious how to generalize a mechanical analysis from polygons to curved parts, especially when this analysis is based
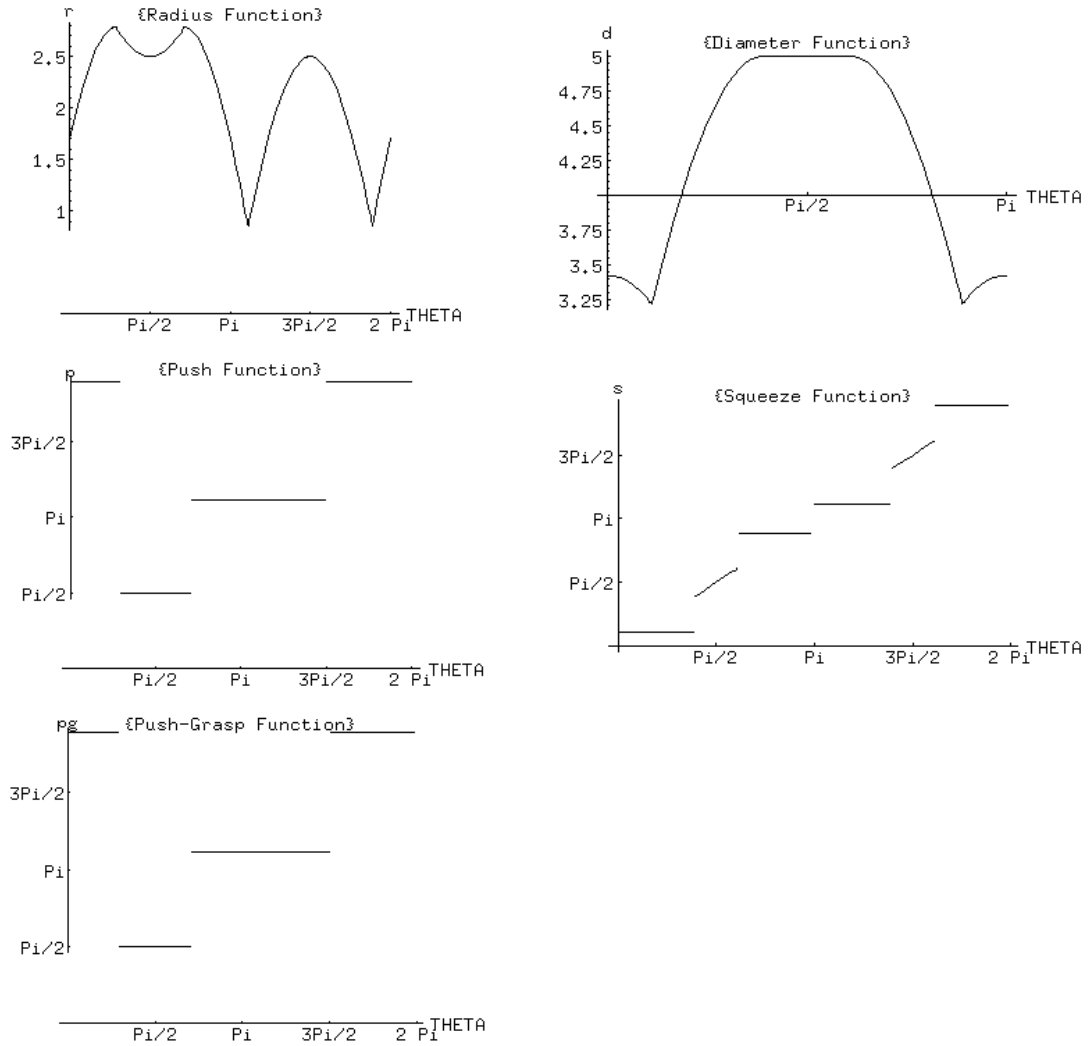
Figure 15: Push-grasp analysis for the pie-shaped part shown in Fig. 16. In particular, notice that while the squeeze-grasp function has period π as before, the push-grasp function has a period 2π. These figures were generated using the system *Mathematica*.

25

Although this upper bound can approach infinity if the part is pushed along a vector from the contact vertex through the part's center-of-mass, we can avoid such actions after the first action causes the part to rotate into one of its stable orientations.

The mechanics of pushing can be captured with an analog to the diameter function [21]. Let a planar part be described with a continuous curve $\mathcal{C}$ in the plane. Let its c.o.m be identified. The distance from the c.o.m to a line in orientation θ tangent to the part varies with θ. Define the *radius function*, $r : S^1 \to \Re$, to record this variation, *i.e.* $r(\theta)$ equals the distance from the c.o.m. to a tangent line of orientation θ. See top of Fig. 15. Notice that unlike the diameter function, the radius function is not necessarily (and except for perfectly symmetrical and homogeneous parts, is not) of period π. The radius function for an n-sided polygonal part or one made up of n linear-circular arcs can be readily computed in time $O(n)$ given the c.o.m. and the ordered sequence of vertices.

The *push function*, $p : S^1 \to S^1$, maps an initial orientation of the part to a final orientation after the push phase. It is a step-ramp function derived from the radius function in the same way that the (squeeze) grasp function is derived from the diameter function. That is, the fixed-point of each step in p is a local minimum in r and discontinuities between steps in p occur at local maxima in r; regions of constant radius become ramps in p. As before, we may consider all steps and ramps as left-closed, right-open. From [2], and analogous to Fact 1, we have:

Fact 2 *Pushing minimizes radius.*

To analyze the mechanics of a push-grasp action, we simply compose the push function with the (squeeze) grasp function to get a function that we call the *push-grasp function* as illustrated in Fig. 15 (for the part shape see Fig. 16).

From Facts 1, 2, the following is clear.

Fact 3 *Push-grasping first minimizes radius, and subsequently diameter.*

For parts made up of n linear/circular arcs, the push and squeeze-grasp functions, p, d, will consist of $O(n)$ steps and ramps (in $[0, \pi)$). Thus, their composition, the push-grasp function can be seen to have only $O(n)$ steps and ramps and can be be computed in $O(n)$ time from p, d (Appendix C). See Fig. 15.

The period of symmetry in the push-grasp function is defined in the same way as that of the squeeze-grasp function Γ was in Equation 2 (Section 2.2). What push-grasping accomplishes wrt squeeze grasping, apart from the mechanical justification, is orienting parts *up to symmetry in their push-grasp function* rather than up to symmetry in their squeeze-grasp function. The latter is always at most π, while the former is almost always 2π. Some exceptions exist: for example, perfectly symmetrical and homogeneous parts (regular polygons) in which even the radius function has symmetry of π or less. Referee 1 pointed out another interesting case: consider a asymmetrical convex-convex thin lens shaped part. The radius function has period of symmetry 2π because of the asymmetry in the lens shape. However, the two local maxima and minima orientations in both the radius and diameter functions match. As a result, the grasp and push functions are identical and hence identical to their composition, the push-grasp function. The push-grasp function has period π and the lens can only be oriented up to symmetry π.

5.1 Planning Sequences of Push-Grasp Actions

The analysis of the planning algorithm, Algorithm A' (Section 4) for squeeze-grasp actions only required that the grasp function be a monotonic function on the set of planar orientations made up of steps with fixed-points and ramps. Since these criteria also apply to the push-grasp function, we can apply the same reasoning to find sequences of push-grasp actions. The planning algorithm is unchanged, except it uses the

24

Figure 14: Modifying Γ into Γ_2 via Γ_1.

each of width y such that $0 < y < x$. Now rotate each subramp about any point in its interior, WLOG the mid-point, into a step. Let us do this for every ramp in $\Gamma_1(Y)$. Let y_0 be the minimum of all these y, $0 < y_0 < x$. Let this modification from Γ_1 lead to a new grasp function Γ_2. Now since every step in $\Gamma_2(Y)$ is of width strictly less than that of the widest step (unless, of course there is a step of width x in $\Gamma_2(Y)$ that is also in $\Gamma_1(Y)$) it is clear that there is an execution of $A'(\Gamma_2)$ that begins with a step of width x that is outside Y (*i.e.* Θ_1 in both $A'(\Gamma_2)$ and $A'(\Gamma_1)$ is the same). Once the first intervals output are the same in both $A'(\Gamma_2)$ and $A'(\Gamma_1)$, and since Γ_2 and Γ_1 are identical within Θ_i (the only changes to Γ_2 from Γ_1 being in Y disjoint from Θ_i), it is clear that an execution of A' on Γ_2 would output the same sequence intervals as it did on Γ_1 culminating in interval Θ_i. Thus we have, $A'(\Gamma_2) = A'(\Gamma_1)$. See Fig. 14.

From the two paragraphs above, we see that there exist executions of A' on Γ, Γ_2 such that $A'(\Gamma_2) = A'(\Gamma)$. Further notice that the modifications made in obtaining Γ_1 and Γ_2 do not affect the period of symmetry T. Thus $A'(\Gamma_2)$ would output the same intervals as did $A'(\Gamma)$ and stop with the output of Θ_i of width less than T. However, notice that Γ_2 is a grasp function made of steps alone and each step has a fixed-point in its interior. By Lemma 3, there is a polygonal part Q that has grasp function Γ_2. The completeness of Algorithm A (Section 3) implies that $A(\Gamma_2)$ would not stop at Θ_i but would continue till an interval of width equal to T was reached. To complete the contradiction, notice that $A(\Gamma_2) = A'(\Gamma_2)$ since Γ_2 is piecewise constant. □

Correctness   Correctness of Algorithm A' refers to the fact that the sequence of intervals output by Algorithm A' lead to a geometrically optimal plan.

The proof of correctness of Algorithm A presented in [14] holds verbatim for Algorithm A'. The main idea is to show that no i-stage plan can collapse an interval larger than Θ_i, the ith interval found by the algorithm. This is proved by induction.

5   Push-Grasp Actions

In this section we relax the assumption that both jaws make contact simultaneously and consider the class of actions that push the part with one jaw prior to grasping, as identified by Brost in [2]. Besides being easier to justify mechanically, this allows us to eliminate, in most cases, the problem of achieving a final orientation only up to symmetry in grasp function.

Let a *push-grasp action* α be the combination of orienting the gripper at angle α wrt a fixed world frame, translating the gripper in direction $\alpha + \pi/2$ for a fixed distance, closing the jaws as far as possible, translating the gripper in direction $\alpha - \pi/2$ for the same distance, and then opening the jaws.

Given sufficient pushing distance, the part will rotate so that one of its edges is aligned with the pushing jaw before the second jaw makes contact. For this class of actions, we substitute two assumptions for Assumption 7 made at the beginning of Section 2.

- The part's center-of-mass (c.o.m.) is given.

- The pushing distance is sufficient to align a stable part edge with the pushing jaw before the second jaw makes contact.

The c.o.m. of a n-sided polygonal part of uniform density is easily determined in $O(n)$ time, given the edges in order, by triangulating the polygon (this can be done in $O(n)$ time for any simple polygon [5]), determining the mass (area) and c.o.m. of each triangle, and combining the results by a weighted sum. A similar approach works for a part made up of n piecewise linear/circular arcs (*GP* parts). The c.o.m for homogeneous algebraic parts of constant height can be determined numerically by integration. An upper bound on the pushing distance can be computed by considering the smallest disk that covers the part [29].

Figure 13: Construction of a polygon compatible with a step function.

the previous step. Let O be the mid-point of this diagonal and it will turn out that O is the centroid of all the parallelograms we construct and also of the final polygon. For the first step $[0, a)$, we can choose LM as any vertical segment and O its mid-point. Define point L' so that $\angle LO\,L' = v - u$ and $\angle L'LO = \frac{\pi}{2} - \alpha + u$. Similarly define M' diametrically opposite to L', and $L'LMM'$ is our required parallelogram. It can be easily verified that this parallelogram is in stable equilibrium when grasped at $\angle \alpha$ and, more generally, that its grasp function agrees with f between orientations $[u, v)$. $L'M'$ is the diagonal to be passed on to the parallelogram of the next step.

Finally, merely translate the k parallelograms (for the k steps in f) so that their boundary forms a polygon as shown in Fig. 13. This is possible since $\sum \angle LO\,L' = \sum (v - u) = \pi$. Moreover, the polygon is convex since each $\angle L'LO$ is less than $\frac{\pi}{2}$. ☐

Remark: If the function f is the grasp function for a triangle then a hexagon is obtained as the part having f as its grasp function by the above procedure. This implies that there may exist several parts having the same grasp function and therefore the same grasp plan can orient any of these parts into a fixed orientation. In fact, there exist infinitely many parts sharing the same polygonal diameter function (and therefore grasp function). A necessary condition by Cauchy's surface formula is that all these parts have the same perimeter (in convex hull). In [37] we present necessary and sufficient conditions for two parts to have the same diameter function.

Lemmas 2 and 3 give us Lemma 4 below. By $A'(\Gamma)$ let us understand the sequence of intervals $\Theta_1, \Theta_2, \ldots, \Theta_i$ output in Step 4 of Algorithm A' upon input of grasp function Γ. Similarly $A(\Gamma)$ is defined.

Lemma 4 *Let Q' be any algebraic part with grasp function Γ'. Then there exists a polygonal part Q with grasp function Γ such that $A'(\Gamma') = A(\Gamma) = A'(\Gamma)$.*

Proof: We modify Γ' into Γ, a grasp function made up of steps alone, as shown in the proof of Lemma 2. Then apply Lemma 3 above to Γ to get Q, a polygonal part, that has grasp function Γ. ☐

The following theorem gives us the proof of completeness.

Theorem 5 *Algorithm A' is complete w.r.t. algebraic parts. That is, it will produce a plan to orient any algebraic part up to symmetry.*

Proof: Let P be the input part with grasp function Γ. Let us use the $O(n)$ time implementation of an iteration of the loop, *i.e.* the box placement implementation described in Section 4.

What has to be proved is that the last interval Θ_i output (in Step 4) will be of width T. Towards a contradiction let, if possible, the algorithm come to a stop when $\Theta_i = [a, b)$ is the last interval returned, $|\Theta_i| < T$ and no other interval Θ of width greater than that of Θ_i exists such that $|\Gamma(\Theta)| < |\Theta_i|$.

Extend $\Theta_i = [a, b)$, say along the right, into an interval $X = [a, c)$ of width T. Let $Y = [b, c)$. The basic idea of the proof that follows is to create a grasp function Γ_2 made up of steps alone such that $A'(\Gamma_2) = A'(\Gamma)$. We first modify Γ within region Θ_i into a grasp function Γ_1 that has only steps in region Θ_i (but could have ramps in region outside Θ_i, *i.e.* in Y). Γ_2 is a modification of Γ_1 converting ramps (if any) in Y into steps. All the modifications performed always preserve the output of A'.

Consider $\Gamma(\Theta_i)$. Let us modify Γ within Θ_i as follows. By Lemma 2 we see that Γ could be modified, within Θ_i (and not changed outside Θ_i), into a grasp function Γ_1 such that $\Gamma_1(\Theta_i)$ contains only steps and that satisfies $A'(\Gamma) = A'(\Gamma_1)$. That is, there *exists an execution* of A' on Γ_1 that would output the same sequence of intervals as it did on Γ and would stop after interval Θ_i was output. Note that $\Gamma_1(Y) = \Gamma(Y)$ (since changes to Γ have been made only within Θ_i) and Γ_1 contains no ramps within Θ_i. See Fig. 14.

Let the largest single step Θ_1 (the first interval output in $A'(\Gamma_1) = A'(\Gamma)$) have width x. Consider a ramp R (if any) in $\Gamma_1(Y)$ between orientations $[a, a + r)$. Let us split R into $1 + \lfloor \frac{r}{x} \rfloor$ equal sized subramps
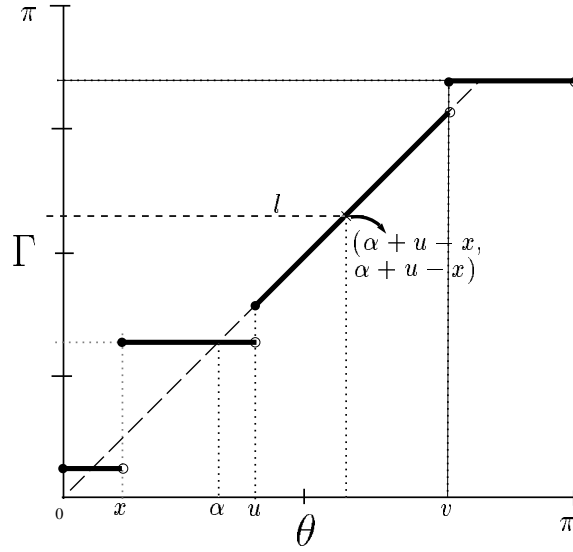
20

Figure 12: Metric upper bound on N, the number of iterations of Algorithm A'.

the reached subset is from a ramp, then notice that *had the grasp function been a step between orientations* $[\phi_0, \phi_2)$, with fixed point anywhere in the interior of the step, *then there exists an execution of this iteration of the main loop that results in the same interval* Θ_{i+1} since the reached subset would be the same: $[\phi_0, \phi_2)$. If Θ_{i+1} is obtained by a top-right placement of the box, we define the reached ramp or step and the reached subset analogously. Let us formalize this paragraph into a lemma.

Lemma 2 *Let the execution of Algorithm A' on a grasp function Γ of a algebraic part P result in intervals* $\Theta_1, \ldots, \Theta_i$ *being output (in Step 4). Then there exists an execution of Algorithm A' on a grasp function Γ' made up of steps alone, that also outputs $\Theta_1, \ldots, \Theta_i$.*

Proof: We change Γ to Γ' as follows. All steps in Γ remain steps in Γ'. Any portion of a ramp that exists in some $\Theta_j, 1 \leq j \leq i$ (*i.e.* this portion has been a reached subset sometime during the execution of A' on Γ), is changed into a step as described in the paragraph above. Finally if a ramp (or portion thereof) does not exist in any Θ_j, it may be "rotated into a step" about any point in its interior (*i.e.* , as before, simply replace the portion of the ramp by a step with fixed point somewhere in the step's interior). Γ' contains steps alone and there exists an execution of Algorithm A' that outputs the same intervals on Γ' as it did on Γ. $\square$

Lemma 3 *Given any piecewise constant function f whose domain and range are the space of orientations S^1, that has period π, and such that each step is of the form $[u, v)$ (i.e. left-closed, right-open: see Appendix B) and contains a fixed-point α of f strictly in its interior (i.e. $u < \alpha < v$). Then there exists a polygonal part Q that has f as its grasp function.*

Proof: We give a construction of polygon Q. Process steps in f from left to right. Consider a single step of f between orientations $[u, v)$. Let the fixed point in this range be α. $u < \alpha < v$ and $\forall \theta \in [u, v), f(\theta) = \alpha$. For every such step we construct a parallelogram that has f as its grasp function *between* orientations $[u, v)$. See Fig. 13. In constructing the parallelogram for this step $[u, v)$, we need a length of one of the diagonals of the parallelogram corresponding to the previous step $[x, u)$. This diagonal (of length d) is a diagonal of the current parallelogram as well. Let LM be this diagonal of length d obtained from the parallelogram of

19

at $(\alpha + u - x, \alpha + u - x)$. See Fig. 12. Therefore the gain in interval length between two iterations is $z = \alpha - x$. If this amount is strictly positive, then the entire ramp can be output in $\frac{v-u}{z}$ iterations. However, $\alpha = x$ and $\beta = y$ are simultaneously possible. In this special case, x, y are semistable orientations. Let $[x_1, x)$ be the ramp immediately before step $[x, u)$. It may be verified that Algorithm A' can include the ramp $[x_1, x)$ in $\frac{x-x_1}{u-x}$ iterations of the main loop. Similar analysis for the ramp $[y, y_1)$ immediately after step $[v, y)$. The ramp $[u, v)$ itself can be included in $\frac{v-u}{z}$ further iterations, where z is the larger of $x - x_1$ and $y_1 - y$.

Thus each ramp corresponds to some z, such that $1/z$ is indicative of the number of iterations to include that ramp. Let z^* be the minimum of all these z. Then $N = O(n^2 + \frac{1}{z*})$.
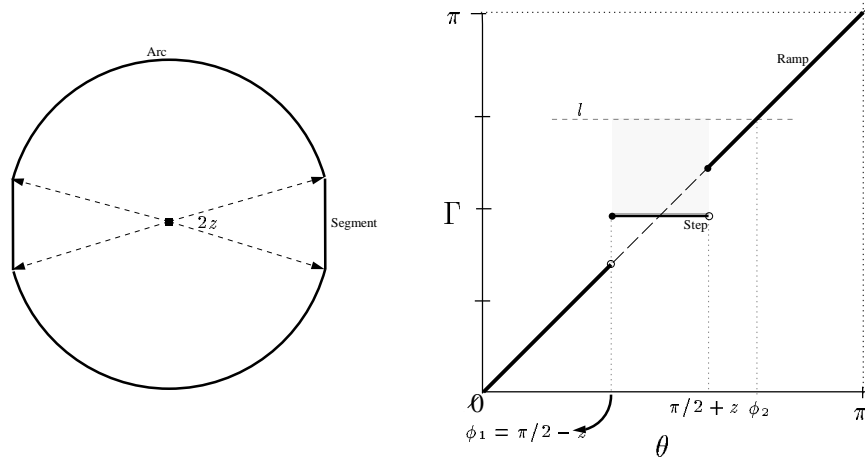

Figure 11: The number of iterations in the main loop of Algorithm A', N, is independent of the number of steps and ramps in the grasp function, n. At the left is a symmetrical curved part bounded by two circular arcs and two straight line segments. The segments subtend an angle $2z$ at the center. At the right is its grasp function consisting of a single step and ramp, the step being of width $2z$. After the first iteration of the Algorithm which finds Θ_1 as this only step, $[\pi/2 - z, \pi/2 + z)$, a box of width $|\Theta_1| = 2z$ is placed as shown. $\Theta_2 = [\phi_1, \phi_2)$ of width $3z$ is computed. The gain in interval length between two iterations is z and the number of iterations is linear in $1/z$. Notice that z can be made arbitrarily small.

4.2 Completeness and correctness

In this section we prove our primary result, namely that for any algebraic part, Algorithm A' will continue to iterate until an interval of width T (period of symmetry in Γ) is output. Our proof requires us to establish a link between the Algorithms A and A' by showing that for every algebraic part, there exists a polygonal part with the same grasp plan. Then we make use of the fact that Algorithm A is complete to show that Algorithm A' is complete for all algebraic parts. Recall the definition of a fixed-point: given a function f, we say that α is a *fixed-point* of f if $f(\alpha) = \alpha$.

First we state and prove a lemma relating the plans for grasp functions containing ramps to those not containing ramps. Let interval $\Theta_{i+1} = [\phi_1, \phi_2)$ be obtained by a bottom-left placement of the box at $(\phi_1, \Gamma(\phi_1))$. See Fig. 11. We refer to the ramp or step to which the point $(\phi_2, \Gamma(\phi_2))$ belongs as the *reached ramp or step* by this placement of the box. Let the left end-point of the reached ramp or step be $(\phi_0, \Gamma(\phi_0))$. In the figure, $\phi_0 = \pi/2 + z$. Then we refer to $[\phi_0, \phi_2)$ as the *reached subset* (of the reached step or ramp). If
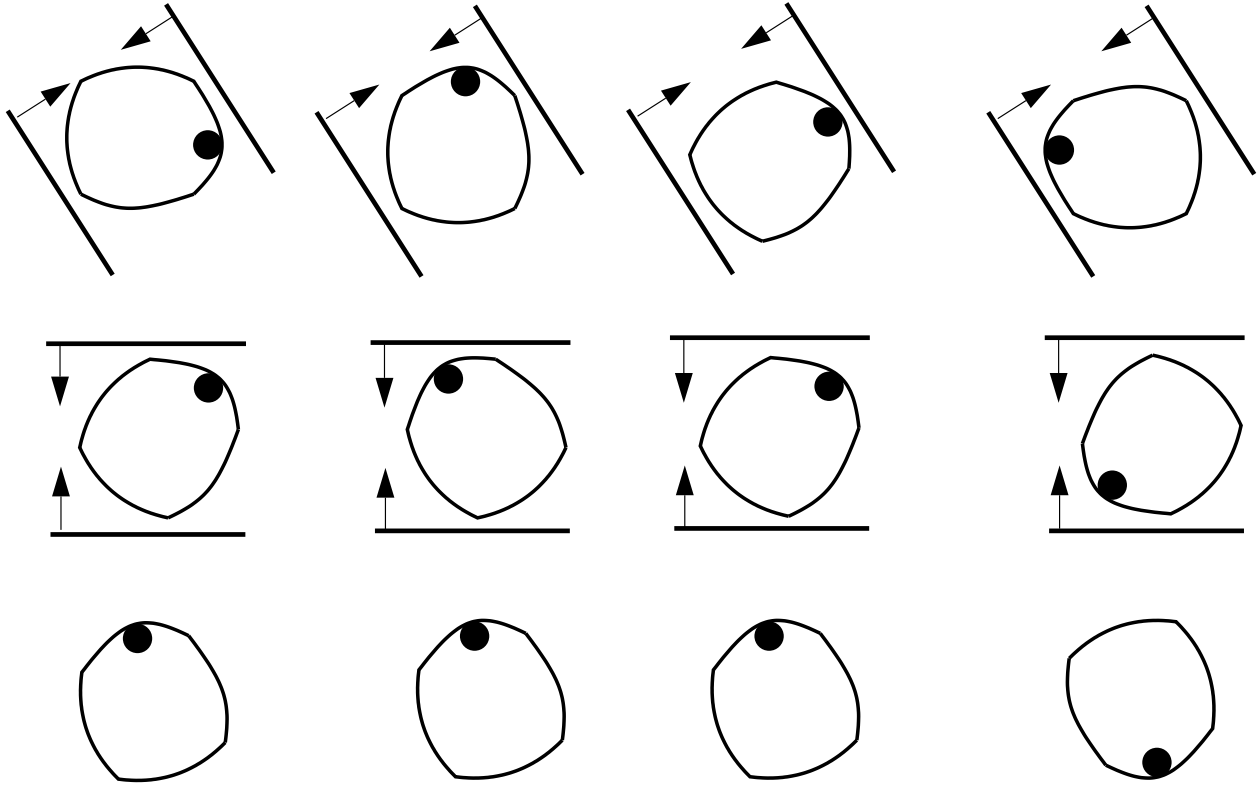
18

Figure 10: Top view of a two-stage plan for orienting the part in Fig. 8 into one of two orientations separated by π. The part is shown with a "registration mark" to help indicate orientation. Four traces of the plan (running from top to bottom) are shown.
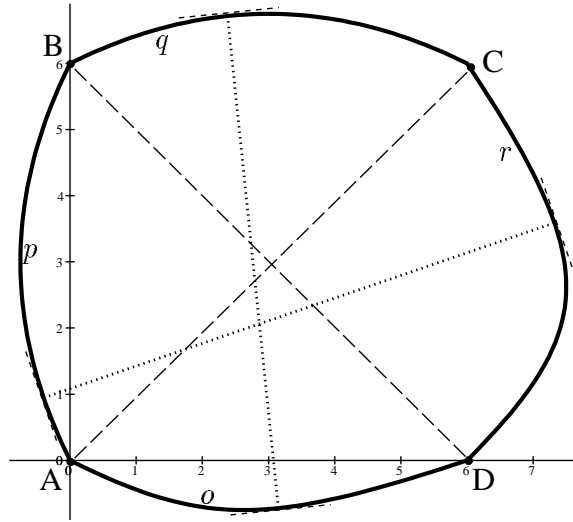
Figure 8: An algebraic part having two maxima and minima in its diameter function. Its convex boundary is made up of four arcs: o, p, q, r and four vertices A,B,C,D. The arcs are cubic parametric curves. The maxima $(\pi/4, 3\pi/4)$ are indicated by dashed lines joining BD and AC. The minima $(5.88°, 108.91°)$ are dotted lines joining points in q, o and p, r. The grasp function is plotted in Fig. 9.
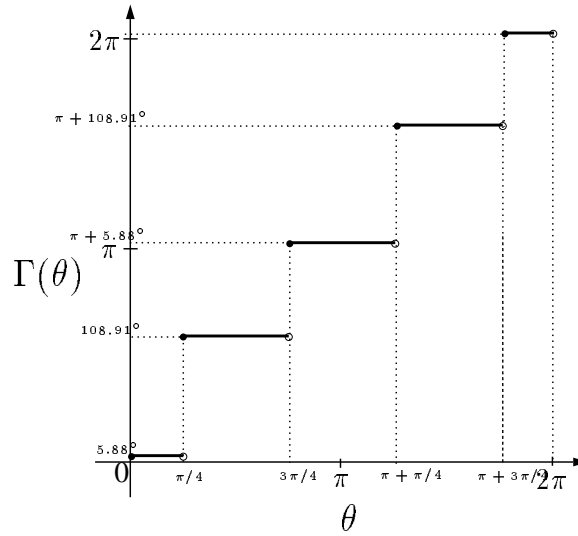

Figure 9: Grasp Function Γ for the part shown in Fig. 8. If θ is the initial orientation of the part wrt the gripper, $\Gamma(\theta)$ denotes its orientation after the grasp. The grasp function has a period of symmetry π, i.e. $\Gamma(\pi + \theta) = \pi + \Gamma(\theta)$. Within a period of symmetry of width π, the grasp function has two steps corresponding to the two minima (and maxima) in diameter function.
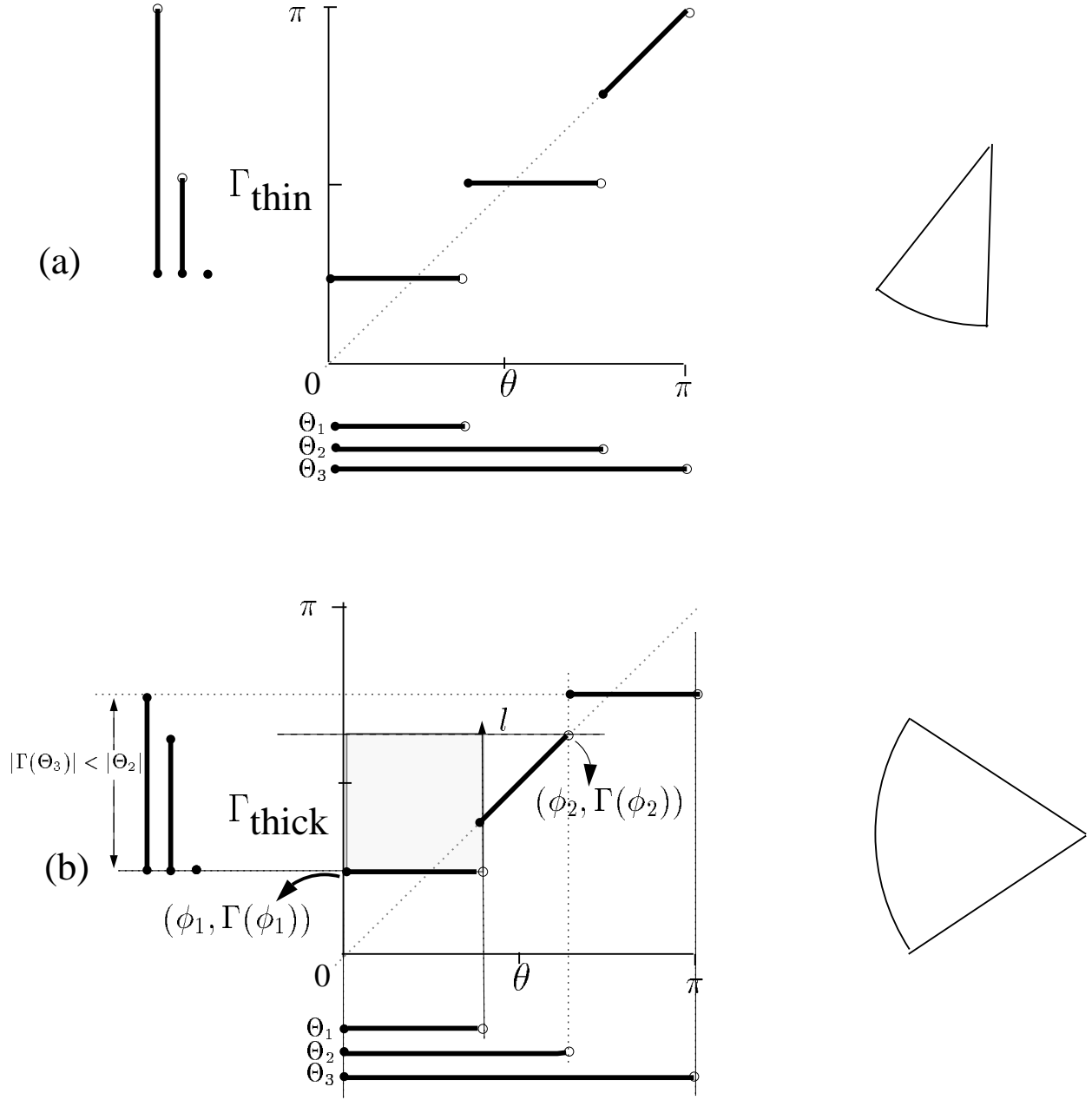
16

Figure 7: Sequence of intervals $\Theta_1, \Theta_2, \Theta_3$ output by Algorithm A' for a thin (in (a)) and thick (in (b)) pie-shaped part (shown alongside to the right in respective zero orientations). The grasp functions each have two steps and a ramp. For the thin slice (half angle $= \pi/9 < \pi/6$), both steps are "taken" before the ramp while for the thick slice (half angle $> \pi/6$) the steps are too far apart to be taken one immediately after the other. Instead, in this case, the ramp has to be included before the second steps.

15

Extend the top of the box into a line l. If l intersects a ramp, let the intersection point be (ϕ_2, ϕ_2). Otherwise, lower until l until it intersects a step or the right end-point of a ramp: $(\phi_2, \Gamma(\phi_2))$. Define the *interval returned by this placement* of the box to be $[\phi_1, \phi_2)$. We repeat this for all possible top-right and bottom-left placements of the box. Set Θ_{i+1} to be the widest of the intervals returned over all placements of the box. See Fig. 7(b) with $i = 1$. The shaded box shown is of width $|\Theta_1|$. The interval returned by this placement is $[\phi_1 = 0, \phi_2)$. This interval is the widest of all box placements and therefore $\Theta_2 = [0, \phi_2)$. See also Fig. 11.

Note that since there are at most $2n$ placements of the box and each placement requires $O(1)$ amortized time, each iteration of the loop takes $O(n)$ time (under the box-placement implementation), n being the number of steps and ramps in Γ. Thus N iterations take $O(nN)$ time.

As in Algorithm A, the sequence of N intervals, $\Theta_1, \ldots, \Theta_N$, can be converted into squeeze grasp actions.

As a numerical example, consider the thin (half-angle = $20°$) pie-shaped part in Fig. 7 again. The discontinuities in Γ occur at $0, 70, 140$ (all orientations in degrees). The fixed-points of the steps are at 50, 90. Θ_1 has been computed as the left most step: $[0, 70)$; $\Theta_2 = [0, 140)$ and $\Theta_3 = [0, 180)$. These intervals result in the grasp actions $\alpha_1 = 80, \alpha_2 = 45, \alpha_3 = 0$ which are precisely the grasp actions (wrt a fixed world frame) shown in Fig. 2.

As another example consider the algebraic part shown in Fig. 8. From the Grasp Function given in Fig. 9, Algorithm A' computes a plan consisting of two grasp actions: the first at $-57.4°$ and the second at 0. The plan for orienting this part is shown in Fig. 10.

4.1   Complexity

In Section 4 we presented a box placement implementation of Algorithm A' that takes $O(n)$ per iteration of the main loop, n being the number of steps and ramps in the grasp function of the part. Thus, if the (optimal) plan output by Algorithm A' consists of N iterations, the complexity of Algorithm A' under the box placement implementation is $O(nN)$. We first show that, for algebraic parts, there need be no upper bound on N in terms of n. However, we provide a bound on N in terms of metric properties. In [35], we present a *measure space* implementation of Algorithm A' that takes $O(n^2 \log n + N)$ time. This implementation is (as good or) better than the box-placement implementation if $N = \Omega(n \log n)$. The details are fairly straightforward and are not presented here.

To show that there is no upper-bound on N in terms of n, let (if possible) there exist a function g, so that $N = O(g(n))$. Consider first the case $n = 4$, the part with two arcs and two segments and 4 vertices, and its grasp function shown in Fig. 11. The intervals returned in Step 4 by Algorithm A' for this part will be such that $|\Theta_i| - |\Theta_{i-1}| = z$ and, therefore the number of iterations for this part, is $\lceil \frac{\pi - 2z}{z} \rceil$ which can be arbitrarily large, *i.e.* z may be chosen so that this quantity is greater than $g(4)$. For general n and g, we can construct an n-vertex part P_n with $n - 4$ vertices being encountered between orientations $(\frac{\pi}{2} - z, \frac{\pi}{2} + z)$. Between these orientations the grasp function would have $O(n)$ steps, and outside this region the grasp function would be a ramp. The number of iterations for this part N_n is $O(\frac{1}{z})$. We can choose z so small that $N_n > g(n)$.

The above paragraph indicates that there cannot be a bound on N as a function of n. However, N is finite (so long as the grasp function is not a single ramp). To see this, we present an upper bound on N in terms of $1/z$. Note that a ramp $[u, v)$ is always surrounded on both sides by steps. Call them $[x, u)$ and $[v, y)$. Let these two steps have fixed-points, α, β, respectively. Consider the step $[x, u)$ with fixed-point α (similar analysis for the other step). Thus, we have $x < \alpha < u$. If a square box of dimension $u - x$ is placed with its bottom-left corner at point $(x, \Gamma(x)) = (x, \alpha)$, then the line l along the top of the box either is over the ramp (in which case the entire ramp in included in one additional iteration) or it intersects the ramp

whose image is smaller than the current interval. This continues until the algorithm finds an interval of length T, the period of symmetry of the grasp function. A plan for orienting the part can be derived from the resulting sequence of intervals.

1. Compute the grasp function.

2. Find the widest single step in the grasp function and let Θ_1 be the corresponding interval, *i.e.* $|\Gamma(\Theta_1)| = 0$. Set $i = 1$.

3. While there exists an interval Θ such that $|\Gamma(\Theta)| < |\Theta_i|$,

   - Let Θ_{i+1} be the widest such interval.
   - Increment i.

4. Set $N = i$. Return the list $(\Theta_1, \ldots, \Theta_N)$.

Algorithm A

The returned list is converted into a sequence of grasp actions (plan) through a formula given in [14].

Theorem 2 *[14] For any polygonal part, Algorithm A finds a plan to orient the part up to symmetry.*

Theorem 3 *[14] For any polygonal part, Algorithm A finds the shortest such plan.*

Theorem 4 *[6] For a polygon of n sides, Algorithm A runs in time $O(n^2)$ and finds plans of length $O(n)$.*

4   Orienting Algebraic Parts

Algorithm A' generates grasp plans for algebraic parts. It does this by explicitly treating ramps in the grasp function. Algorithm A' follows the general structure of Algorithm A, *i.e.* given the grasp function of a *polygonal* part, Algorithm A' finds the same plan as would Algorithm A. We assume Γ has at least one step (otherwise P has a constant diameter function[2] with $T = 0$. Thus P is trivially oriented up to symmetry in Γ).

For algebraic parts, we modify the semantics of the term *interval*. Recall that Algorithm A referred to an interval as any set $[u, v)$ such that both u, w are points of discontinuity in Γ (local maxima in d). In Algorithm A', however, there are two kinds on intervals $[u, v)$: *fixed* and *variable*. Fixed intervals are those with both u, v as points of discontinuity in Γ or end-points of ramps. Variable intervals are those with one of u, v as a point of discontinuity (end-point of a step) in Γ or end-point of a ramp, while the other is a point *somewhere* along the interior of a ramp. We do not need to consider intervals Θ such that both of its end-points lie on ramps since such intervals will satisfy $|\Gamma(\Theta)| = |\Theta|$ and are thus useless from the point of view of Algorithm A'.

Consider an iteration of the main loop (Step 3). Given, Θ_i, computing Θ_{i+1} may be done as follows. Place an axis-parallel square box of dimension $|\Theta_i|$ with its bottom-left corner at the left end-point of a step or ramp in the grasp function. This is called a *bottom-left* placement. Top-right placements are analogous. Let a bottom-left placement be defined at the point $(\phi_1, \Gamma(\phi_1))$.

---

[2]Constant diameter curves other than circles are popular in classical geometry, where they are known as *gleichdicke*, orbiforms, or spheroids [4].
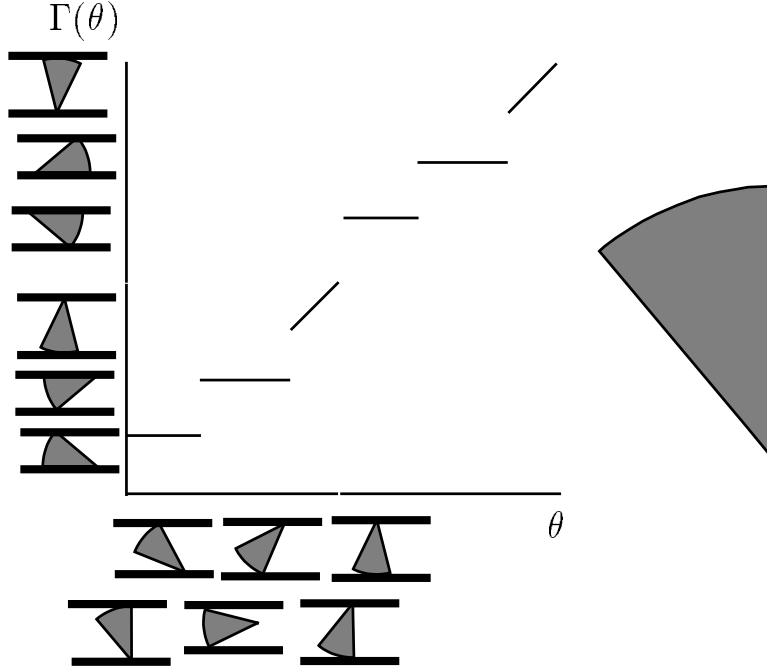
Figure 6: Grasp function from diameter for a pie-shaped part shown on the right in zero orientation.

Periodicity in the grasp function gives rise to *aliasing*, where orientation θ is indistinguishable from orientation $\theta + T$. Any sequence of actions that maps θ to θ' will map $\theta + T$ to $\theta' + T$. This implies that there is no sequence of gripper actions that can map orientations θ and $\theta + T$ into a single final orientation.

For a given part, let T be the smallest period in its grasp function. We say that a plan orients a part *up to symmetry* if the set of possible final orientations includes exactly $2\pi/T$ orientations that are equally spaced on S^1. For example, for a part with no rotational symmetry, a squeeze plan orients the part up to symmetry if the plan yields exactly two final orientations that are π radians apart. A part with 3-fold rotational symmetry can be oriented up to symmetry with a squeeze plan that yields six possible final orientations each $\pi/3$ radians apart.

After the part is oriented up to symmetry, we can regrasp once more to achieve a grasp at some offset from this set of orientations.

3   Algorithm A

To establish terminology for our treatment of algebraic parts in the next section, we we briefly review the planning algorithm for polygonal parts [14] which we call Algorithm A. We define an *interval* in the domain of a grasp function is a semiclosed continuous subset of S^1 of the form $[a, b)$ such that a, b are points of discontinuity in the grasp function. For an interval Θ, let θ refer to the leftmost point in the interval and $|\Theta|$ be its Lebesgue measure. The *convex hull* of a set $\Theta \subseteq S^1$, denoted by $\mathrm{HULL}(\Theta)$, is the smallest connected set that contains Θ. We define the *image of a set* Θ to be the convex hull of the set $\{\Gamma(\theta)|\theta \in \Theta\}$ and refer to it by $\Gamma(\Theta)$.

As summarized below, Algorithm A works backward from a single final orientation, finding a squeeze action that collapses an interval of orientations into this final orientation. It then searches for a larger interval

This directly follows because the jaws are continuously moving towards each other while in contact with the part (Assumptions 5-9 at the beginning of Section 2) and that the diameter of the part at any intermediate orientation is the distance between the jaws at that instant. The final orientation is a local minimum of the diameter function. Further squeezing would violate rigidity of the part. The grasp function as defined here is properly called the *squeeze-grasp function* (to distinguish it from the *push-grasp function* defined in Section 5).

For polygonal parts, the diameter function is piecewise sinusoidal [33, 37] and therefore there are no regions of constant diameter. From the continuity of d, if $u, v \in S^1$ are any two consecutive local maxima in d, then there has to exist a local minimum $\alpha \in S^1$, such that $u < \alpha < v$. Then, $\forall \theta \in (u, v), \Gamma(\theta) = \alpha$ by Fact 1. Further, we have that for $\Gamma(u) = u, \Gamma(v) = v$. However, by a simple modification to the grasping process as described in Appendix B, we may assume that for every local maximum $u, \Gamma(u) = \alpha > u$, where α is the smallest local minimum greater than u. Thus, we may say that $\forall \theta \in [u, v), \Gamma(\theta) = \theta$. This is done for every pair of consecutive local maxima u, v.

Therefore, it may be observed that for polygonal parts, the grasp function Γ is piecewise constant. Each of these constant pieces $[u, v)$ is referred to as a *step*. The unique local minimum between u and v, namely α, is the *fixed-point* of the step $[u, v)$ since $\Gamma(\alpha) = \alpha$. Every step is left-closed and right-open. The only discontinuities in Γ are at the local maxima orientations in d. There are at most $2n$ steps in the grasp function of a polygonal part of n vertices. See Fig. 13 for an example of a grasp function of a polygonal part.

For algebraic curved parts it is possible to have regions of constant diameter. Regions of non-constant diameter in d are converted to steps in Γ as before. Now, let interval (u, v), be a (maximal) region of constant diameter in d. Following Fact 1, corresponding to (u, v), we get $\forall \theta \in (u, v), \Gamma(\theta) = \theta$. We call each such interval as a *ramp*. Again, from an argument that will be described in Appendix B, we may assume that ramps are also left-closed and right-open. Consider an example of the derivation of Γ from d in Fig. 4. Regions $[0, \theta_1)$ and $[\theta_1, \theta_3)$ are steps while $[\theta_3, \pi)$ is a ramp. See Fig. 6 for the final grasp function.

The grasp function Γ of any algebraic part is thus made up of steps and ramps, the only points of discontinuity in Γ being local maxima in d and possibly end-points of regions of constant diameter. Appendix A presents a classification of orientations in terms of grasp stability giving an intuitive perspective on these critical orientations. Fig.s 7,11 give further examples of grasp functions of curved parts.

To rule out pathological parts that might result in grasp functions with infinite steps, the following theorem is presented that states that algebraic parts have finite grasp functions. Its proof follows directly from Lemma 1 and the derivation of Γ from d presented above.

Theorem 1 *The grasp function Γ of an algebraic part is made up of a finite number of steps and ramps.*

2.2   Orienting a Part *up to Symmetry*

We noted that the grasp function has period π due to symmetry in the gripper; rotating the gripper by 180 degrees produces a symmetric arrangement that preserves the diameter. Rotational symmetry in the part also introduces periodicity into the grasp function. The grasp function has period T if for all $\theta \in S^1$,

$$\Gamma(\theta + T) = (\Gamma(\theta) + T) \bmod 2\pi. \tag{2}$$

Polygons with r-fold rotational symmetry have period $T_r = 2\pi/(r(1 + r \bmod 2))$ in grasp function. For example, a part with no rotational symmetry ($r = 1$) has a grasp function with period π. An equilateral triangle has 3-fold rotational symmetry; its grasp function has period $\pi/3$. A square has 4-fold rotational symmetry; its grasp function has period $\pi/2$.
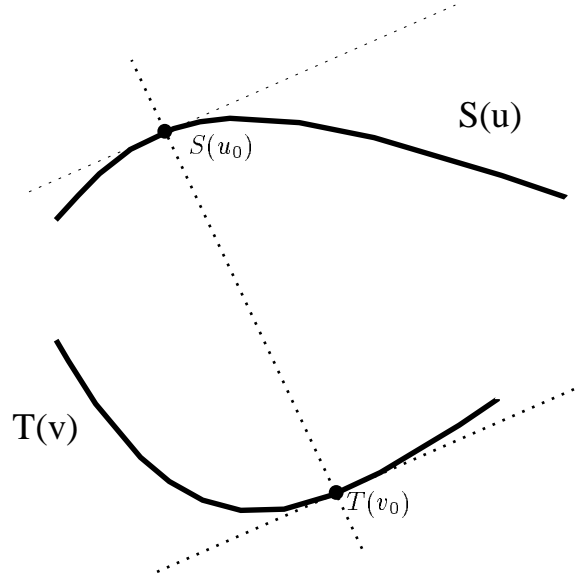
Figure 5: Pairs of curve segments $S(u), T(v)$. If $S(u_0), T(v_0)$ define an extremum orientation, then they satisfy the system of equations 1 (but not vice versa). This implies that the following three lines coincide: the normal to $S(u)$ at u_0; the normal to $T(v)$ at v_0; the line joining u_0 and v_0.

Thus, the only resulting change is a different system of algebraic equations from Eqns. 1. The property of finiteness of the number of solutions is clearly unchanged. Parametric curve segments have the advantage that testing whether the solution lies in the curve segment is easy: simply check if the bounds for the parameter (in our case: between 0 and 1) are met.

2. $u_0 \in \{0, 1\}, 0 < v_0 < 1$ (and vice versa: interchanging u_0, v_0). Let $u_0 = 0$. Then via a similar technique, we can show that v_0 has to be the solution of an algebraic equation which can have at most $3(\kappa + 1)$ solutions. Thus, this type of extrema are at most $12s^2(\kappa + 1)$ in number.

3. $u_0, v_0 \in \{0, 1\}$. The number of such u_0, v_0 pairs are clearly $4s^2$. Many of them will not form extrema (geometric conditions can prune out such extrema).

Therefore, in all there are at most $s^2(18\kappa^2 + 66\kappa + 52)$ extrema in the diameter function of $\mathcal{P}$. $\square$

2.1.2 The Grasp Function

Notice that the orientation θ of P wrt G is not changed between the non-contact and contact states. It is only after the contact state that it is possibly changed and the *grasp function* Γ records this change (see Fig.s 3,4,6).

$\Gamma : S^1 \to S^1$ is defined so that if θ denotes an orientation of P wrt to G in the contact state, $\Gamma(\theta)$ denotes the orientation in the grasped state. Notice that $\Gamma(\theta + \pi) = \pi + \Gamma(\theta)$, *i.e.* the function Γ has period π due to symmetry in the gripper (see equation 2 in Section 2.2). The orientation $\Gamma(\theta)$ is also referred to as the *image* of orientation θ. We now show how to derive Γ from d.

Fact 1 *(Squeeze) Grasping minimizes diameter.*

10

Proof: We show that the diameter function of an algebraic part contains a finite number of extrema (local maxima and minima). This implies that the number of regions of constant diameter cannot be infinite because between any pair of them has to lie an extremum orientation (from continuity of d). Also, since d is clearly differentiable except at these critical points, the lemma follows.

Recall that P is made up of s piecewise smooth algebraic curve segments. P's diameter function has a finite number of extrema. We may dispose of extrema defined by linear segments since there are at most s of them. Other extrema (and indeed, other orientations: due to convexity of P) are defined by two distinct points on the curved boundary.

Let an extremum orientation θ_0 be defined by two points $S(u_0), T(v_0)$ on the curved segments S, T. $S = T$ is possible; we need to then look for solutions in which $u_0 \neq v_0$ (we may ensure that no orientation is defined by two points on the same arc segment by making every arc "small enough" with the addition of pseudo vertices). For simplicity (see remark below) we assumed that S and T are represented in rational parametric form, $S(u), T(v)$, where the parameters u, v vary between 0 and 1 to trace out the segment. Let $X_S(u)$ denote the rational algebraic expression representing the x-coordinate of $S(u)$. The polynomials X_T, Y_S, Y_T are similarly defined. Recall that κ is the maximum degree in the polynomials appearing in these algebraic expressions taken over all curve segments. There are three cases to consider.

1. $0 < u_0, v_0 < 1$. That is, the extremum orientation is formed by points that lie to the interior of two smooth curve segments.

   Consider the bivariate function $D^2(u, v)$ to be the square of the Euclidean distance between $S(u)$ and $T(v)$. That is,

   $$D^2(u, v) = (X_S(u) - X_T(v))^2 + (Y_S(u) - Y_T(v))^2.$$

   Note that
   $$\frac{\partial(D^2)}{\partial u} = 2\left(X_S(u) - X_T(v)\right)\frac{dX_S}{du} + 2\left(Y_S(u) - Y_T(v)\right)\frac{dY_S}{du}$$

   is well defined for $0 < u, v < 1$ (since S is smooth). Similarly $\frac{\partial(D^2)}{\partial v}$ is well defined in this region.

   The key observation is that since θ_0, the orientation defined by $S(u_0), T(v_0)$ is a local extremum orientation in d, (u_0, v_0) will be a local extremum in $D^2(u, v)$. To see this, consider an ϵ-neighborhood around the point (u_0, v_0), ϵ sufficiently small: all points in this neighborhood will result in a D^2 value less (more) than $D^2(u_0, v_0)$ if θ_0 is a local maximum (minimum). See Fig. 5 for a geometric interpretation.

   In other words, u_0, v_0 is a solution of the system of equations:

   $$\frac{\partial(D^2)}{\partial u} = 0; \quad \frac{\partial(D^2)}{\partial v} = 0. \tag{1}$$

   There can be at most $18(\kappa + 1)(\kappa + 2)$ simultaneous solutions to this system and as a result, at most $18(\kappa + 1)(\kappa + 2)$ extremum orientations can be defined by the interior of the curves S, T. Adding such "curve-interior" extrema over all curve segment pairs, we get a bound of $18(\kappa + 1)(\kappa + 2)s^2$.

   Remark: If the underlying curve equations for S, T are known only implicitly as $f_S(x, y) = 0$, $f_T(x, y) = 0$, then the above analysis still holds: an orientation defined by the pair of points $(x_0, y_0), (x_1, y_1)$ is extremal only if $f_S(x_0, y_0) = 0$; $f_T(x_1, y_1) = 0$; $\frac{df_S}{dx}(x_1 - x_0) + \frac{df_S}{dy}(y_1 - y_0) = 0$; $\frac{df_T}{dx}(x_1 - x_0) + \frac{df_T}{dy}(y_1 - y_0) = 0$. The solution obtained must then be tested for arc-inclusion.
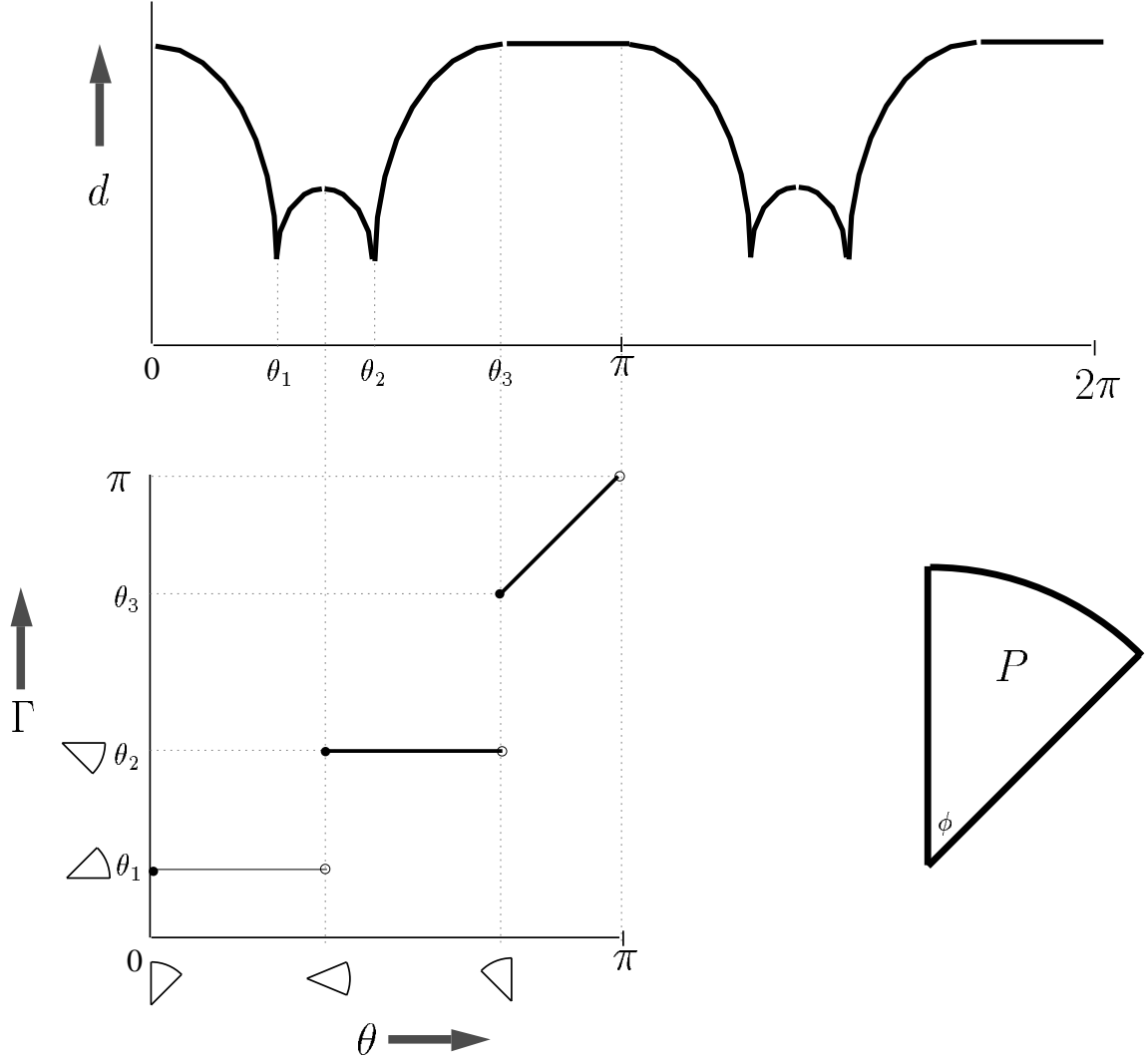
9

Figure 4: **(top)** The diameter function for the pie-shaped part (shown at the bottom-right). The part is a circular sector of angle ϕ. Therefore, $\theta_2 - \theta_1$, the difference between the local minima, is ϕ, which is also equal to the measure of the constant diameter interval, $\pi - \theta_3$. **(bottom)** The grasp function is shown for the portion $[0, \pi)$. During a squeeze-grasp action, the part rotates so as to reduce the diameter, terminating when the diameter reaches a local minimum. The constant diameter region becomes a ramp in the grasp function and other regions turn into steps.
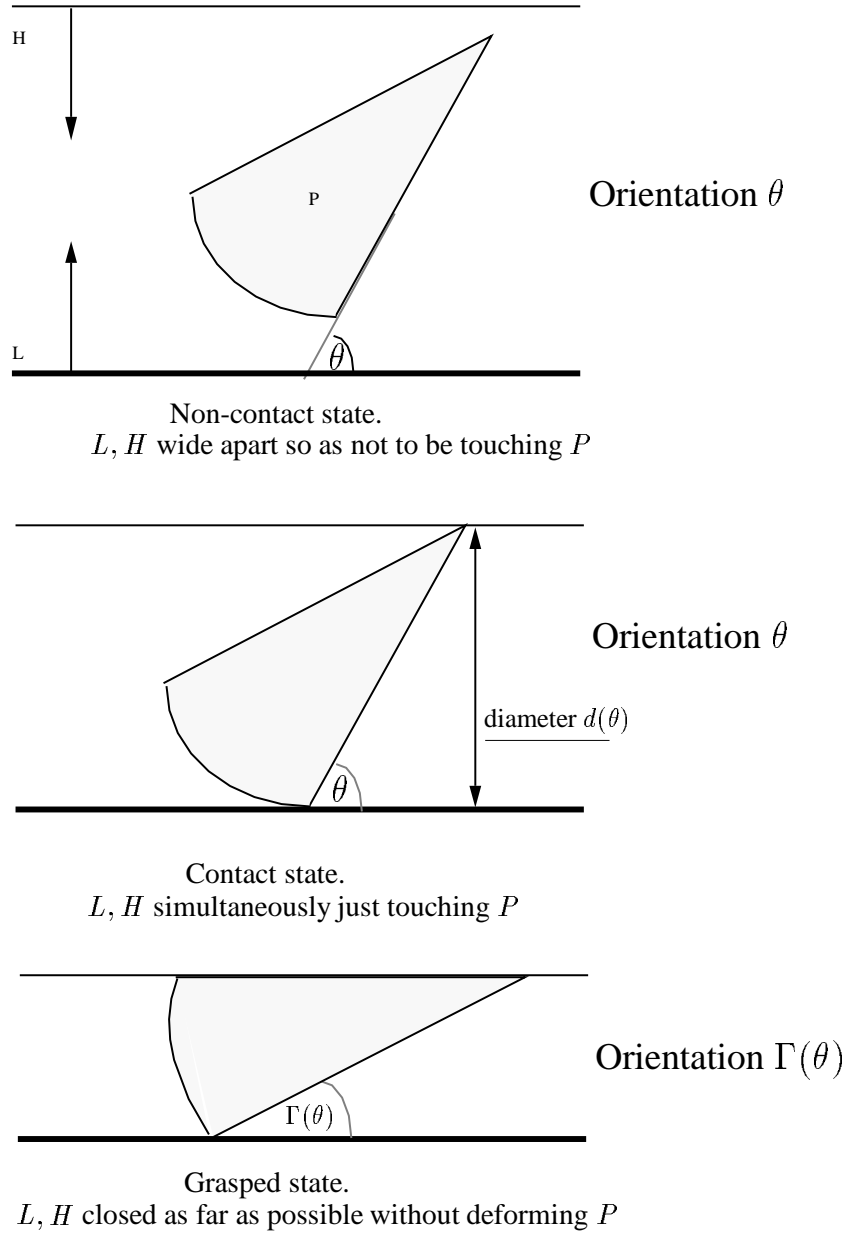
8

Orientation θ

Non-contact state.
L, H wide apart so as not to be touching P

Orientation θ

diameter $d(\theta)$

Contact state.
L, H simultaneously just touching P

Orientation $\Gamma(\theta)$

Grasped state.
L, H closed as far as possible without deforming P

Figure 3: Configurations of the part P wrt the gripper G during the grasping process. In the non-contact state **(top)**, the jaws *L,H* are not touching P. In the contact state **(middle)**, both jaws just touch P but do not effect its orientation θ. Between the contact and grasped state **(bottom)**, the orientation of P changes to $\Gamma(\theta)$, Γ being the part's grasp function.

7

An orientation of P with respect to the gripper is *defined* by the boundary points of P in contact with G.

- The *grasped state*: After contact, L and H move towards each other, continuously changing the orientation of P wrt to G, as far as possible without deforming the part.

6. All part (and gripper) motion occurs in the plane.

7. L, H make contact simultaneously with the part.

   We refer to such grasps as *squeeze-grasps*. This can almost never be achieved without sensors. In Section 5, we consider another class of actions, *push-grasps*, that are easily mechanically justifiable. This assumption of pure squeezing is made only to simplify exposition of the proof of plan existence and planning algorithm; these can then be applied in generating push-grasps as well.

8. All motion is slow enough that inertial forces are negligible [22, 29].

9. Once contact is made between a jaw and the part, the two surfaces remain in contact throughout the grasping motion. The action continues until further motion would deform the part.

10. There is zero friction between the part and the jaws [13].

2.1 Diameter and Grasp Functions

Let S^1 denote the set of planar orientations and $\Re_+$ the positive reals.

2.1.1 The Diameter Function

Consider the part and gripper in planar projection. The diameter function $d : S^1 \to \Re_+$ of a part is defined in terms of its planar projection. Let P be in an orientation θ with respect to G such that P, G are in the contact state. See Fig. 3. The *diameter of P at orientation θ*, $d(\theta)$, is defined to be the distance between the jaws L, H in this contact state. See Fig. 4. Convexity theory [43] defines width functions for 3D objects which become the diameter function as defined above for 2D parts.

The following properties of the diameter function can be verified:

- The diameter function is continuous: $\Delta d \to 0$ as $\Delta \theta \to 0$. It is single valued and positive with domain S^1 [43].

- The diameter function of a part is equal to the diameter function of its convex hull (since only points on the convex hull are accessible to the jaws of the gripper).

- The diameter function has period π. This is because L, H can be interchanged in the definition.

- Let p denote the perimeter of the projection P. Then

$$\int_0^\pi d(\theta) \; = \; p.$$

This follows from Cauchy's formula restricted to 2D (see Problem 22.14 on page 173 in [1]).

Lemma 1 *The diameter function of an algebraic part is differentiable at all but a finite number of points in S^1 and it contains a finite number of local maxima, local minima, and regions in S^1 of constant diameter.*

6

functions is also uncountably infinite since they cannot be partitioned into equivalence classes as they can for polygonal parts. Therefore, the results of Natarajan and Eppstein cannot be applied to algebraic parts.

The grasp function of a algebraic part is constructed from another function, the *diameter function* (see Section 2.1.2). Jameson [17] used this function to show that any two-dimensional convex body must have at least two stable equilibria where it can be grasped between parallel jaws. The maximum value in the diameter function of a part is known as the *diameter* of the set of points describing the part and is a well-known concept in Computational Geometry [8]. In classical geometry the diameter function is also known as the *width* function [43]. An exact characterization of diameter functions for polygonal parts can be found in [37].

In [31], we presented a linear-time parallel mesh-connected computer algorithm for planning grasps of polygonal parts. In [36], we considered the class of *generalized polygonal* (GP) parts, whose boundaries contain only linear and circular arcs. This paper generalizes these results to the broader class of algebraic parts.

2   Mechanical Analysis

Let $\mathcal{P}$ denote the part and P, the convex hull of its planar projection. Let G be a *parallel jaw gripper*, such that jaw motion is orthogonal to the contacting faces. Let L and H denote the lower jaw and higher jaw of G, respectively. We assume:

1. $\mathcal{P}$ is rigid.

2. The convex projection P is known and is composed of s segments of planar *algebraic* curves (with rational parameterizations).

   A planar algebraic curve is the set of zeros of a polynomial $f(x, y)$. The equation $f(x, y) = 0$ is referred to as the *implicit* representation of the curve. The *parametric* representation of a planar curve (in a parameter t) is a set of two equations $x = g_1(t), y = g_2(t)$. Further, if g_1, g_2 are ratios of two polynomials, it is a *rational* parameterization. Conics and most other algebraic curves used in engineering posses a rational parameterization.[1]

   The assumption of rational parametric curves (used in Lemma 1) is only for simplicity as the analysis can be easily extended to include implicit forms. Let constant κ refer to the maximum degree over all the polynomials that appear in the rational parameterizations of the s curves.

3. The part is presented in isolation; we do not address the related problem of isolating parts from a bin (commonly known as *singulating*).

4. The part's initial position is unconstrained as long as it lies on a horizontal surface somewhere between the two jaws. The part remains between the jaws throughout the grasping.

5. G is in only one of these three states wrt to P (see Fig. 3).

   - The *non-contact state*: L, H could be wide apart so that G is not touching P.
   - The *contact state*: L, H could be simultaneously "just touching" P (without changing the orientation of P).

---

[1]However, not all algebraic curves do. Noether's theorem states that an algebraic curve $f(x, y) = 0$ possesses a rational parameterization if and only if f has genus zero. A curve genus measures the difference between the number of double points of f and the maximum number of double points a curve of the same degree as f can have [16].

to resist arbitrary forces and torques on the part. Each contact provides a *wrench*: a force with a point of application. In the plane, a wrench can be represented as a vector in $\Re^3$, where the first two components represent the direction of force and the third component represents a moment about an arbitrary origin [27]. A set of planar wrenches provides form closure if they positively span $\Re^3$. Results from linear algebra show that at least four wrenches are necessary for form closure. Recently, [20] showed that four wrenches are sufficient for any piecewise-smooth compact connected planar body, excluding surfaces of revolution.

Jameson [17] was one of the first to analyze the static stability of parts grasped with the parallel-jaw gripper. As with point contacts, the quality of a grasp depends on the orientation of the part with respect to the gripper. To allow for bounded uncertainty in orientation, Wolter [42] proposed a grasp metric based on the angular uncertainty that can be tolerated before a polygonal part switches to a different stable configuration. Brost [2] incorporated a model of frictional wedging and gave an algorithm for removing this uncertainty using controlled sliding during grasping.

The analysis of controlled sliding for manipulation was pioneered by Mason [21]. The difficulty is that the motion of a pushed part on a planar surface with friction depends on the distribution of pressure on this surface. In his dissertation, Mason showed that the *sign* of the rotation rate is independent of the distribution of pressure and depends only on the relative position of the part's center of mass. [3, 10, 32] develop graphical methods for determining the set of all possible motions that can occur due to contacts with Coulomb friction. Peshkin [29] quantified Mason's result using a minimum-work principle to bound the set of all possible rotation centers of a pushed part. Recently, Lynch [18] developed a graphical representation of all possible instantaneous motions of a sliding part when it is pushed by a single planar jaw. His analysis considers both kinematic and force constraints and can be used to identify motions that maintain edge contact between the part and the pusher.

Fearing [12] considered the planar motions of parts due to two moving point contacts. He showed that bounded slip could be useful for resolving angular uncertainty and for manipulating parts using a third fingertip to move parts from one stable pose to another. Toward the end of his paper, Fearing noted that if parts were allowed to slip "without feedback from the hand, part orientation and position are not known". In contrast, [14] and the current paper show that slip can in fact be used to determine part orientation (and position! [25]).

Trinkle and Paul [41] used controlled slip to gain an enveloping grasp of a part initially in contact with a flat support surface. They considered parts moving in the vertical plane due to squeezing contacts with a two fingered hand. They showed how to find contacts for fingers both with and without friction that will force the part to lift off the support surface. They also showed how to partition the boundary of a curved object into "liftability segments" based on an algebraic representation of contact normals. Using Peshkin's minimum power principle, they showed how to plan trajectories that will subsequently slide parts into the palm of the hand. Although their planning algorithm was demonstrated only for convex polygonal parts, the grasp functions described in this paper have a similar flavor to Trinkle and Paul's analysis of liftability segments for curved parts. We also employ slip to reorient parts and to achieve a desired grasp. Our approach, however, is to plan a sequence of motions that will eliminate substantial uncertainty in the orientation of curved parts.

The idea of using a sequence of pushing or grasping motions to reduce uncertainty in part orientation has been addressed by [19, 24, 30, 40]. Although each of these planning algorithms use realistic models of mechanics, each used heuristics to search for plan strategy, none of which are guaranteed to find a plan in polynomial time. Natarajan [26] ignored the mechanics of parts feeders and focused on the computational problem of planning with a given set of grasp functions. For polygonal objects with a finite number of stable orientations, he presented planning algorithms that are polynomial in the the number of edges and the number of grasp functions. The complexities of his algorithms were improved by Eppstein [9]. For algebraic parts, there can be an uncountably infinite set of stable orientations. Furthermore, the set of relevant grasp
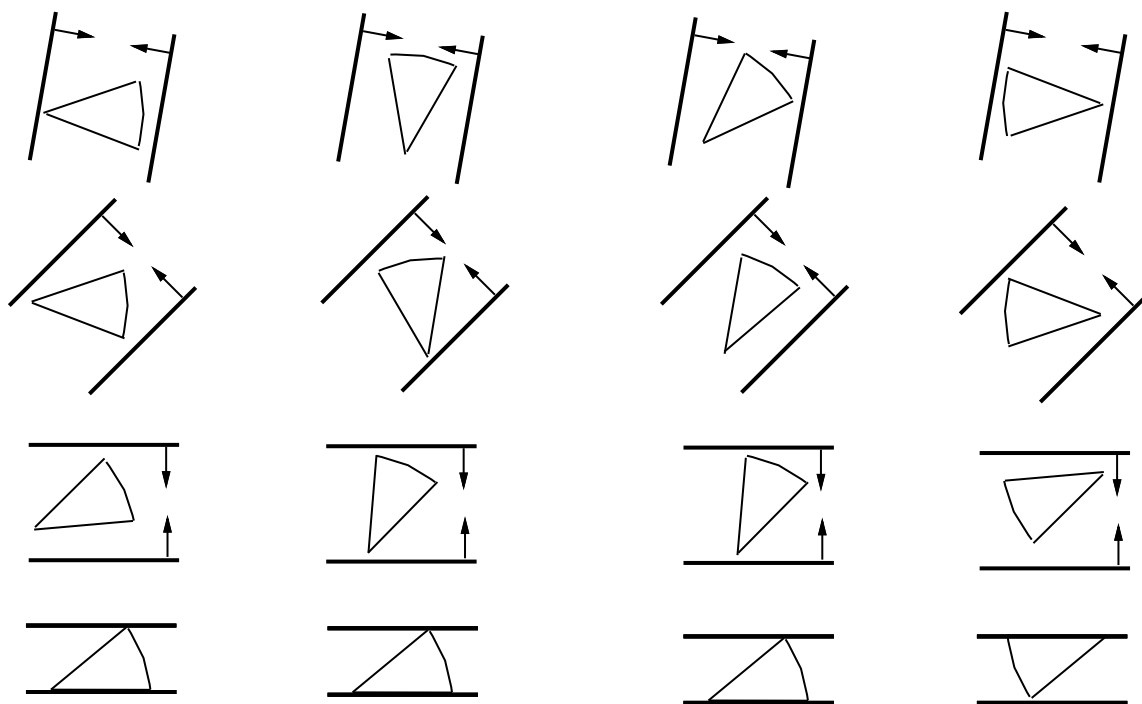
Figure 2: Top view of a three-stage plan for orienting a pie-shaped part with half angle $20°$ into one of two orientations. Four traces of the plan (running from top to bottom) are shown. Note that the part's initial orientation is different in each trace (top of each column). The gripper orientation at each stage, indicated by two parallel-lines, is the same for each trace; yet the same desired grasp configuration is achieved in all cases. To obtain a single final orientation, push-grasp actions may be used. See Fig. 17.

Many industrial parts contain curved edges: a polygonal approximation of a curved part does not provide a reliable model of mechanical behavior. For example, whereas polygonal parts always rotate into one of a small finite number of stable orientations when grasped, this cannot be guaranteed for algebraic parts. Treating the uncountable set of possible outcomes requires significant extensions to the algorithm and proof of completeness developed for polygonal parts.
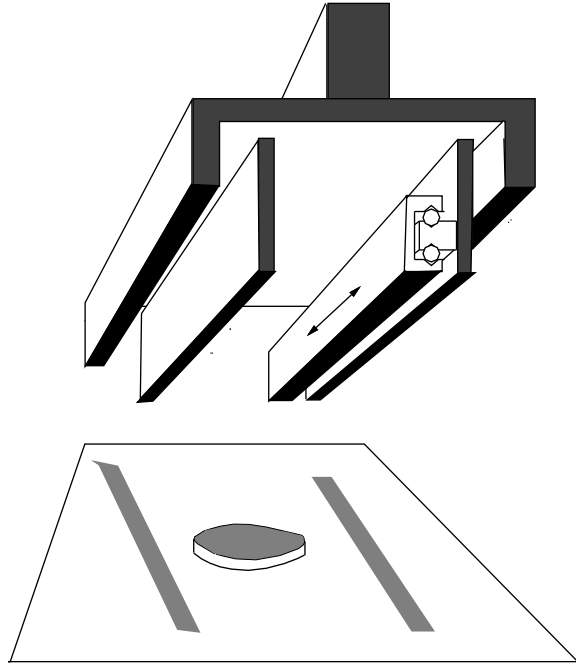

Figure 1: Schematic of a modified parallel jaw gripper above an algebraic part.

We assume that there is zero friction between the part and the jaws in the plane of the part, but high friction resisting forces out of the plane. This can be justified at low cost by mounting a linear bearing on one jaw as described in [13]. Each *grasp action* is the combination of orienting the gripper at angle α wrt a fixed world frame, closing the jaws as far as possible over the part without deforming it, and then opening the jaws. Note that this can be accomplished with a binary pneumatic valve; no external sensing is required.

The resulting part motion can be characterized by a "grasp function" that maps initial to final orientations of a given part after a single grasp. We characterize these functions for algebraic parts and give an algorithm that takes a grasp function as input and generates a grasp plan that orients a part up to symmetry in its grasp function. We then prove that a grasp plan exists for any algebraic part.

The planning algorithm requires time $O(n^2 \log n + N)$, where n is the number of segments in the grasp function and N is the length of the plan produced. To show that N is finite, we give a polynomial bound on N based on the grasp function.

1.1   Related Work

There is a substantial literature on the subject of robot grasping. See [15] and [28] for reviews. The *quality* of a grasp can be defined in many ways depending on hand geometry and the class of parts being grasped. The definition of *form closure* [38] captures the intuitive notion of a good grasp. A set of contacts provides form closure if infinitesimal part motion is completely constrained; equivalently, the set of contacts is able

Manipulating Algebraic Parts in the Plane[*]

Anil S. Rao[†]and Kenneth Y. Goldberg[‡]

December 7, 1993

Abstract

When manipulating parts, it is important to determine the orientation of the part with respect to the gripper. This orientation may not be known precisely or may be disturbed by the act of grasping. It is in some cases possible to use mechanical compliance to orient parts *during* grasping. It was recently shown [14] that any part with polygonal boundary can be oriented and grasped in this manner using a parallel-jaw gripper.

Many of the curves currently used in engineering design are *algebraic* but non-linear. Although these curves can be approximated as polygons for the purpose of visualization, such approximations can lead to false conclusions about mechanical behavior. In this paper we consider the class of parts whose planar projection has a piecewise algebraic convex hull.

Our primary result is a proof that a grasp plan exists for any such part. We give a planning algorithm that produces the shortest plan and runs in time $O(n^2 \log n + N)$, where n is the number of transitions in the grasp function and N is the length of the plan produced. We believe this to be the first paper to address the problem of manipulating algebraic parts when their initial orientation is unknown.

1 Introduction

To manipulate a part into a desired final position and orientation (pose), a standard approach is to sense the part's initial pose, plan and execute a grasping motion, and then move the part into the desired final pose. Methods for sensing and grasping comprise entire sub-fields within the field of Robotics. We have been exploring how a particularly simple mechanism, the parallel-jaw gripper, can be used to manipulate a broad class of parts.

In previous work, we proved that any polygonal part can be oriented up to symmetry using a sequence of gripper motions [14]. We assume that the part's shape is known and that its motion is restricted to the plane; thus we treat the planar projection of the part. In this paper we consider the class of parts whose planar projection has a piecewise algebraic convex hull. We call these *algebraic* parts. We note that if the surfaces of a solid part are algebraic, the convex hull of its planar projection must also be algebraic. An example is illustrated in Fig.s 1 and 2.

Fig. 2 illustrates the grasp plan for four initial orientations of the part. In this case three open-loop grasping motions are sufficient to align the part with the gripper. Our primary result is a (constructive) proof that such a grasp plan exists for any algebraic part.

[*]This research was supported in part by NSF award IRI-9123747 and by ESPRIT Basic Research Action No. 6546 (Project PRoMotion). This is a revised version of a paper submitted to the IEEE Transactions on Robotics and Automation in August 1992 under the title: "Grasping Curved Planar Parts with a Parallel-Jaw Gripper".

[†]Department of Computer Science, Utrecht University, Padualaan 14, Postbus 80.089, 3508 TB Utrecht, Netherlands. anil@cs.ruu.nl, Tel: 31-30-535093, FAX: 31-30-513791.

[‡]Institute of Robotics and Intelligent Systems, Department of Computer Science, PHE 204, University of Southern California, Los Angeles, California 90089-0273. goldberg@iris.usc.edu, Tel: 1-213-740-9080, FAX: 1-213-740-7877.